Technische Universität München

Klinik für Kinderkardiologie und angeborene Herzfehler des

Deutschen Herzzentrums München des Freistaates Bayern

Increased Wall Shear Stress may be determining the Development of Ascending Aortic Dilatation in Patients with Bicuspid Aortic Valve

Eike Philipp Schneider

Vollständiger Abdruck der von der Fakultät für Medizin der Technischen Universität München zur Erlangung des akademischen Grades eines

Doktors der Medizin

genehmigten Dissertation.

Vorsitzender: Univ.-Prof. Dr. E. J. Rummeny

Prüfer der Dissertation:

1. Univ.-Prof. Dr. J. Hess, PhD
2. Univ.-Prof. Dr. K.-L. Laugwitz
3. Univ.-Prof. Dr. R. Lange

Die Dissertation wurde am 05.04.2012 bei der Technischen Universität München eingereicht und durch die Fakultät für Medizin am 29.01.2014 angenommen.

Dedication

To My Mother.

Contents

List of Abbreviations

2D	- Two dimensional
3D	- Three dimensional
4D	- Time-resolved three dimensional / four dimensional
AAo	- Ascending Aorta
AHA	- American Heart Association
AoV	- Aortic valve
AI	- Aortic insufficiency
AS	- Aortic stenosis
AVR	- Aortic valve replacement
BAV	- Bicuspid aortic valve
BCT	- Brachiocephalic trunk
BSA	- Body surface area
CFD	- Computational fluid dynamics
CHD	- Congenital heart disease
Cm /sec	- Centimetre per second
CMR	- Cardiovascular magnetic resonance
CoA	- Coarctation of the aorta
DAo	- Descending aorta
e. g.	- For example
ECG	- Electrocardiography
ECM	- Extracellular matrix
HG	- Quicksilver

HTN	- Hypertension
OSI	- Oscillatory shear index
m^2	- Square metre
mm	- Millimetre
MS	- Marfan syndrome
m /sec	- Meter per second
MMP	- Matrix-metallo-proteinase
min	- Minutes
PA	- Pulmonary artery
P_{blood}	- Blood pressure
$P_{systole}$	- Systolic blood pressure
$P_{diastole}$	- Diastolic blood pressure
RF	- Regurgitation fraction
SMC	- Smooth muscle cells
TAA	- Thoracic aortic aneurysm
TAV	- Tricuspid aortic valve
TUM	- Technische Universität München
WSS	- Wall shear stress
WSS_{axial}	- Axial wall shear stress
WSS_{circ}	- Circumferential wall shear stress
$WSS_{magnitude}$	- Magnitude of wall shear stress

1 Introduction

1. 1 Background and Aim of this Study

The author would like to comment on the ongoing discussion about aortic vessel disease in patients with bicuspid aortic valve (BAV). Furthermore he wants to link this issue to the obvious importance of blood flow and its attributed role in the development of vascular pathologies. Additionally, this chapter shall explain the purpose of the study as well as back up the theory of wall shear stress (WSS) and the latest features in applied imaging tools.

"Cardiology is flow" (Richter, Edelman 2006, page: 2679).

Richter and Edelmann used this title in 2006 for their pleading that blood flow should be more seriously focused on as it has a driving role in physiology and pathology of the human cardiovascular system.

Besides its vital physiological importance for the human organism and the developmental impact on formation of vessels and the heart itself (Bremer 1932, pages: 1-2; Hinrichsen 1990, pages: 209, 259; Bolton 2005, pages: 1, 85; Richter, Edelman 2006, page: 2679; Goerttler 1955, pages: 41-45), blood flow and flow forces are also well known to be a ruling factor responsible for the origin of several pathologies of the cardiovascular system, above all atherosclerosis (Cheng et al. 2006, pages: 2745-2747). But also aneurysmal vessel disease (Shojima et al. 2004, pages: 2502-2504) or pulmonary vascular remodelling (Botney 1999, page: 361) are affected.

Paradoxically, blood flow which is driven and maintained by the heart and the blood delivering vessels also seems to play an important role in aetiology of cardiovascular diseases. Flow forces like pressure and shear are natural physiological phenomena. However, like blood pressure also shear stress may become pathological under certain conditions (Malek et al. 1999, page: 2036). Nevertheless, pathophysiology in this field is still not fully understood.

Therefore, during the last four decades scientific attention was more and more often paid to the impact of hemodynamic stress on vascular remodelling (Caro et al. 1969, abstract; Ku et al. 1985, pages: 293, 300; Cheng et al. 2002, pages: 2745-2747). But even though, blood pressure monitoring, function analysis and volumetric flow estimations are part of clinical routine, especially in congenital

heart disease (Wood 2006, pages: 605-606; Varaprasathan et al. 2002, page: 904; Fratz et al. 2008, pages: 3-6; Pennell et al. 2004, page: 1940-1965), still, shear stress quantification does not belong to daily practice as Richter and Edelmann correctly determined (Richter, Edelman 2006, page: 2679).

A possible reason for that might have been the inability to reliably measure shear in vivo (Stalder et al. 2008, page: 1219). However, concentrating on flow force calculation researchers could at least experimentally show that one must differentiate between decreased and increased wall shear metrics as the following sections will show.

Decreased hemodynamic shear forces appear to cause atherogenesis in arterial vessels, such as the coronary arteries (He, Ku 1996, page: 81), the carotids (Zarins et al. 1983, pages: 506-511) or the abdominal aorta (Pedersen et al. 1999, pages: 330-332). One can say, that this theory is nowadays generally accepted since several in vitro and in vivo studies have well and comprehensively shown that specifically lowered and oscillatory shear forces cause atherosclerotic plaque growing (Ku et al. 1985, page: 300; Zarins et al. 1983, page: 511; Nerem 1992, page: 279; Malek et al. 1999, page: 2036-2037; Wentzel et al. 2005, page: 853; Cheng et al. 2006, page: 2747). Summarizing, decreased WSS has a huge impact on atherosclerosis. Some locations like vessel branches, bifurcations or tight curves are prone for plaque growing as those anatomical spots cause flow disturbances and thereby altered shear forces (Malek et al. 1999, page: 2036).

Besides atherosclerotic lesions, also development and progress of vessel widening is highly discussed to be influenced by flow shear forces. Yet, in this case, increased wall shear stress is thought to be an important factor for the development of arterial dilation, aneurysm or even dissection (Xu et al. 2009, page: 300; Tse et al. 2011, page: 834); apart from others like arterial hypertension (HTN), smoking, inflammatory diseases or predisposing genetic syndromes (ACCF/AHA/AATS/ACR/ASA/SCA/SCAI/SIR/STS/SVM 2010, page: e 75).

Basically, this idea is not new. Di Guglielmo reviewed post-stenotic aortic aneurysms “as result of mechanical factors” already in 1955 (Di Gugliemo, Guttadauro 1955, pages: 440-442). Kim et al stated in 1992 that high WSS may slowly initiate wall changes which finally lead to formation of aneurysm (Kim et al. 1992, pages: 112, 115, 116). In 2009, Xu et al. linked high wall shear stress with “accelerated metabolism in aortic aneurysm wall” (Xu et al., 2009, page: 295). Just recently, Luo et al investigated higher shear stress values at the neck of re-canalized cerebral aneurysms suggesting that increased levels of haemodynamics may play a substantive role in aneurismal recurrence (Luo et al. 2011, page: 752). And Tse et al argued that elevated wall shear stresses might be associated with extension of aortic aneurysms (Tse et al. 2011, page: 834).

The same way certain anatomical areas may cause lowered shear stress, other regions in the vascular tree may lead to elevated velocities coming along with enhanced shear stress, e.g. aortic stenosis (AS) (Holman 1954, page: 116) congenital malformations like coarctation of the aorta (CoA) (Rao 2005, page: 426) and also bicuspid aortic valves (Robicsek et al. 2004, pages: 181, 184).

However, due to the lack of routine diagnostic tools the impact of increased flow velocities and shear forces in aneurysmal vessel disease is still intensively debated. Especially the discussion about aortic dilation in BAV, *figure 1*, is far away from having found consensus.

But, during the last twenty years, implementing features in functional cardiovascular magnetic resonance (CMR) brought unique new possibilities. Today, modern CMR permits to receive complex data of vascular haemodynamics. Now it is possible to generate in vivo time-resolved three dimensional (4D) visualisations of blood flow in several regions of the human cardiovascular system (Kilner et al. 1993, pages: 2238-2239; Frydrychowicz et al. 2007, page: 261; Wetzel et al. 2007, pages: 434-435; Hope et al. 2010, page: 56). The group around Markl from the Department of Medical Physics at the University of Freiburg im Breisgau, Germany, was able to generate remarkable in vivo 3D visualizations of both normal flow patterns in healthy volunteers and severely changed flow fields in cardiovascular disease (Markl et al. 2011, pages: 6-10).

These striking 3D images from only slightly to very strongly altered flow lead automatically to the assumption that changed flow patterns and acting shear forces may have been generally underestimated and give the discussion about shear stress in aneurysm a new drive. Concerning the existence of such heavily altered flow profiles, regarding direction and intensity of flow, like the studies above revealed, one must conclude that the question of decreased or increased WSS is not the only one. Obviously, the direction of wall shear stress matters as well.

Ku and He performed in vitro wall shear stress studies in 1985 and 1996, respectively, and recognized similar 3D shear stress properties in smaller vessels. Taking this in account, they defined an oscillatory shear index (OSI) considering the temporal amplitude and the changing direction of shear stress (Ku et al. 1985, page: 296; He, Ku 1996, page: 79). For the first time, not only axial WSS seemed to be important. This was logical as WSS is the result of friction forces acting in all three spatial dimensions. In laminar flow the dominating component is axial shear stress (WSS_{axial}), in the direction of flow. Yet, assuming from the previously mentioned complex flow patterns other components, as circumferential WSS (WSS_{circ}), might be of importance as well, *figure 2 and 3*.

However, measuring wall shear stress in vivo has remained a challenging task.

A new approach using four dimensional CMR (4D CMR) introduced by Stalder et al in 2008 was an enormous improvement in this context. With the purpose to generate vectorial flow and shear metrics they developed a new technique which allows for estimating in vivo time-resolved 3D wall shear stress values over complete arterial sections (Stalder et al. 2008, pages: 1219, 1221).

This opened numerous new opportunities in assessing acquired cardiovascular diseases like aortic regurgitation or stenosis, but also congenital malformations like CoA (Frydrychowicz et al. 2008, pages: 402-403; Markl et al. 2009, pages: 776-777).

As already mentioned, particularly dilation of the ascending aorta (AAo) in patients with BAV is still passionately discussed (Ward 2000, pages: 81-84; Braverman et al. 2005, pages: 500-503). This topic is of interest for several fields of medicine. Cardiologists, heart surgeons and, above all, paediatric cardiologists are eager to reach more insights into this complex medical problem.

Until today, two main controversial explanations for aortic vessel disease in BAV are debated. These opposing points of view advocate either an inborn connective tissue disease or dilation of the AAo secondary to altered blood flow patterns (Fedak et al. 2003, page: 904; Bauer et al. 2006, page: 220). The second theory argues that changed flow caused by BAV might lead to aortic dilation throughout life time. Supporting the latter view, recent data from our group have shown that flow patterns in BAV patients are helically altered and significantly differ from those in individuals with tricuspid aortic valve (TAV) (Meierhofer et al. 2010, poster presentation).

Basing on these findings and given the newest possibilities in in vivo WSS measurement using 4D CMR, the purpose of this work was to compare shear stress acting upon the ascending aorta in BAV and TAV. This was performed within the actual discussion of ascending aortic vessel disease in BAV patients. To the author's knowledge this study is the first one investigating in vivo WSS in the AAo of two age and sex matched populations with either BAV or TAV.

1. 2 Bicuspid Aortic Valve (BAV)

BAV belong to the most frequent congenital heart diseases (CHD) (Braverman et al. 2005, page: 470) and play a role in many fields of medicine, like paediatric cardiology, cardiology, heart surgery and pathology. There are numerous studies highlighting this topic from a lot of different points of view (Roberts 1970, page: 72-83; Basso et al. 2004, pages: 661-663; Ward 2000, pages: 81-85; Bauer et al. 2007, pages: 485-490).

Thus, the author will only give a short review of the most relevant facts concerning BAV.

Morphology of BAV has often been described. The earliest description of BAV known was contributed by Leonardo da Vinci about 400 years ago (Mills et al. 1978, page 951). Principally, the malformation presents with two unequally sized cusps as one leaflet results from merging of two smaller ones (Braverman et al. 2005, page: 473). Fusion has been described in all variations. However, their distribution is not equal. Merging of right and left coronary cusp (type 1, *figure 1*) appears to be the most often found pattern, whereas type 2 is less often and type 3 just rarely seen, *figure 1*, (Braverman et al. 2005, pages: 473-475; Schaefer et al. 2008, page: 1636). Fernandez et al. suggested in 2009 that BAV with different leaflet orientations might be distinct entities (Fernández et al. 2009, pages: 2314-2317): However, this theory has not been proved in human studies yet.

Unfortunately, nomenclature of BAV subtypes still varies strongly according to either cusp alignment with regard to the coronary arteries or anterior-posterior localizing of the leaflets (Roberts 1970; page: 79; Cripe et al. 2004, page: 139). For the present study typecasting of Schaefer et al. from 2008 was chosen (Schaefer et al. 2008, page: 1636). *Figure 1* gives an overview of the different types of BAV according the cusp alignment of the aortic valve.

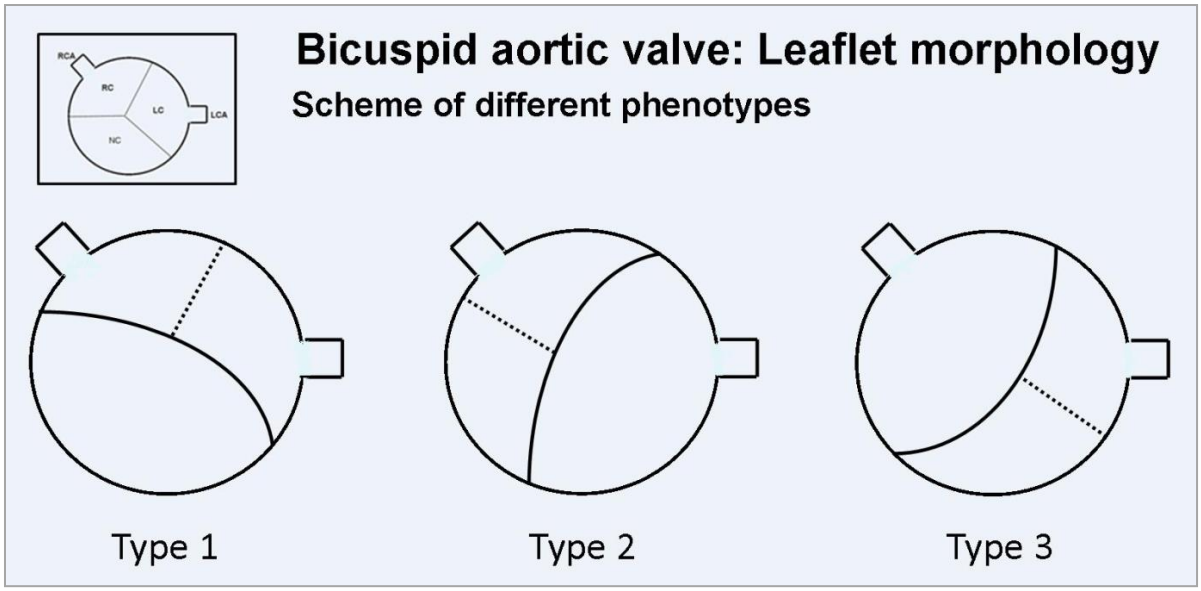

Figure 1: BAV leaflet morphology; view: parasternal, short axis. Small panel on top left presents reference scheme of TAV; BAV, three different types in the row: type 1 - fusion of right and left cusp, type 2 - fusion of right and non-coronary cusp, type 3 - fusion of left and non-coronary cusp. Pointed lines depict raphes of fusion ridge which might be seen sometimes. RC = right coronary cusp, LC = left coronary cusp, NC = non-coronary cusp. RCA = right coronary artery, LCA = left coronary artery. Modelled after Schaefer (Schaefer et al. 2008, page: 1636).

Incidence of BAV is mostly ranked between 0.5 - 2 % of the population (Roberts 1970, page: 78; Basso et al. 2004, page: 663; Fedak et al. 2003, page: 900). The occurrence of BAV can be sporadic or familial (Huntington et al. 1997, page: 1811; Cripe et al. 2004, page 142), however *NOTCH1* gene

mutations which “may trigger (…) valve calcification” in BAV have been found in both familiar and sporadic cases (Mohamed, Aherrahrou 2006, pages: 1460, 1463-1464). Even though, BAV can be an isolated defect different investigators found that it is also often associated with other cardiac malformations like CoA, Turner’s syndrome, ventricular septal defect, persistent ductus arteriosus, William’s syndrome, Shone’s syndrome or coronary anatomic variants (Braverman et al. 2005, pages: 480-481).

As BAV are frequently associated with aortic stenosis (AS), aortic insufficiency (AI), infective endocarditis, dilation, aneurysm or even dissection of the ascending aorta they have such a deep medical impact (Hahn et al. 1992, page: 286; Ward 2000, page: 84) requiring intensive medical and surgical treatment. Facing that and hereditary of BAV, regular surveillance of patients and screening of their first degree relatives is indicated (Siu, Silversides 2010, pages: 2794-2795; McBride, Garg 2011, page: 1194).

The first case of a dilated AAo in association with a BAV was described by Reid in 1952 (Reid 1952, pages: 628-629), before other pathological studies by Edwards and Roberts contributed more data in the following decades (Edwards et al. 1978, page: 1025; Roberts, Roberts 1991, pages: 714-716). Ever since, especially dilation in the proximal to middle AAo is object of discussion since their cause is still unknown (Braverman 2011, page: 508).

It appears to be evidenced that histological abnormalities of the ascending aortic wall are the reason for their weakness guiding to dilation or even more fatal complications like dissection or rupture (Bonow 2008, page: 112). The misnomer cystic media necrosis has often been used to name the histopathological situation in aortic wall tissue behind BAV (ACCF/AHA/AATS/ACR/ASA/SCA/SCAI/SIR/STS/SVM 2010, page: e 39). But, since no cysts and only rare necrosis can be found this synonym is outmoded today (Child, John S. in Braverman et al. 2005, page: 504). Still, structural abnormalities in the AAo of BAV patients are present. The 2008 AHA guidelines summarize these under the term “disorder of vascular connective tissue” (Bonow et al. 2008, page: e559). The abnormalities reach from smooth muscle cell (SMC) apoptosis (Bonderman et al. 1999, page: 2142) over elevated matrix-metallo-proteinase (MMP) activity (Koullias et al. 2004, page: 1102) to elastic fragmentation (de Sa et al. 1999, page: 590) and death-promoting mediator expression (Schmid et al. 2003, page: 541).

Even though, all studies mentioned above are lacking of a plausible presentation of a cause-effect relation between tissue abnormalities and aortic dilation, most of them automatically argue with an inborn wall defect as the major cause for aortic pathology in BAV.

One of the few defending the second, minor supported theory of “poststenotic dilation”, the influence of haemodynamic forces as an eventual reason for aortic dilation in BAV patients, is Gunteroth. He fortifies that the “type of turbulence” may matter, though without providing any evidence (Guntheroth 2008, pages: 108-109). Yet, the new imaging and shear force measuring methods alluded in section 1.1 could reveal new insights in flow and shear force properties behind bicuspid aortic valves and let this theory experience a renaissance.

1. 3 Wall Shear stress and Oscillatory Shear Index

This study was designed to specifically research wall shear metrics in the AAo of BAV patients and to compare them to a healthy control population.

1. 3. 1 Wall Shear Stress (WSS)

Haemodynamic forces of blood flow in vessel lumen can roughly be subdivided into two principles units: first, blood pressure, which imposes stretching to the vessel wall and, second, shear stress, a frictional force acting on the vessel (Botney 1999, page: 363).

Fluids can be subject to shear stress when they are viscous. Proceeding from the assumption that blood is a Newtonian fluid, i.e. it presents a linear relation between shear stress and shear rate, it displays viscosity. The friction stress of blood flow on a boundary, e.g. a vessel wall, is named wall shear stress (Stalder 2009, pages: 46, 48-49).

“The arterial wall shear *stress* is the frictional force acting on unit area of the vessel wall and is equal to the product of the viscosity coefficient and the wall shear *rate;* the wall shear rate is equal to the velocity gradient at the wall”(Benson et al. 1980, page: 568).

$$\vec{\tau} = \mu \frac{dv}{dh} \qquad (1.3)$$

Where τ is the shear stress vector, μ is the viscosity of the fluid, V the velocity along the area and h the height (the radius in a tube formed vessel) at the boundary (Stalder 2009, page: 53). Note that this equation considers only one dimension, e.g. wall shear stress in anterograde direction. But the

tangential shear stress vector at the wall, WSS, can be separated into its axial (**WSS** $_{axial}$) and circumferential components (**WSS** $_{circ}$), *figure 1.*

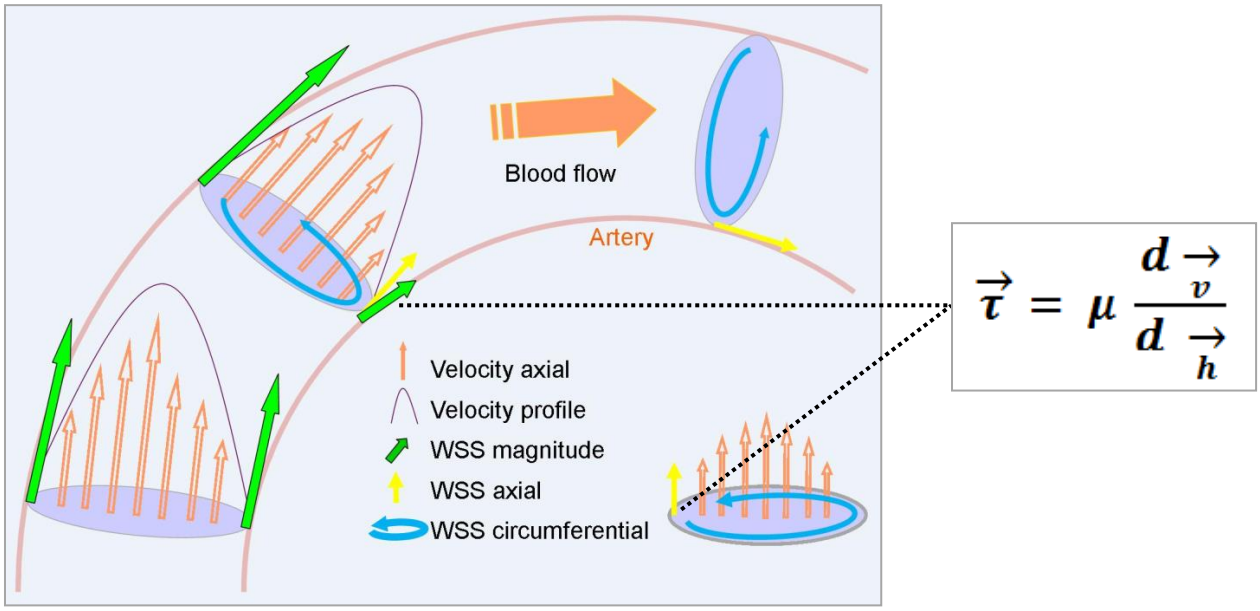

Figure 2: Blood flow illustration in a bent vessel with acting shear stress components: WSS = wall shear stress. Displayed are the components of WSS (axial and circumferential), the vector of WSS magnitude as a result of flow and flow profiles. WSS $_{magnitude}$ in a bent tube like the aorta is higher in the outer curvature then at the inner side (green arrows).

However, the vectorial nature of blood flow is three dimensional and the same counts for wall shear stress. The relation of WSS and three-directional velocity vectors is given by:

$$WSSmag = II \underset{WSS}{\longrightarrow} II = \sqrt{(WSS\ axial)^2 + (WSS\ circ)^2} \quad (1.4)$$

Where **WSS** $_{mag}$ is a scalar of the experimental WSS vector $\overrightarrow{\mathbf{WSS}}$, (Stalder 2009, page: 74), *figure 2.*

WSS is widely accepted as a promoting factor in atherosclerotic plaque growing (Chiu, Chien 2011, abstract). However, its global impact on the development of aortic disease is still poorly understood.

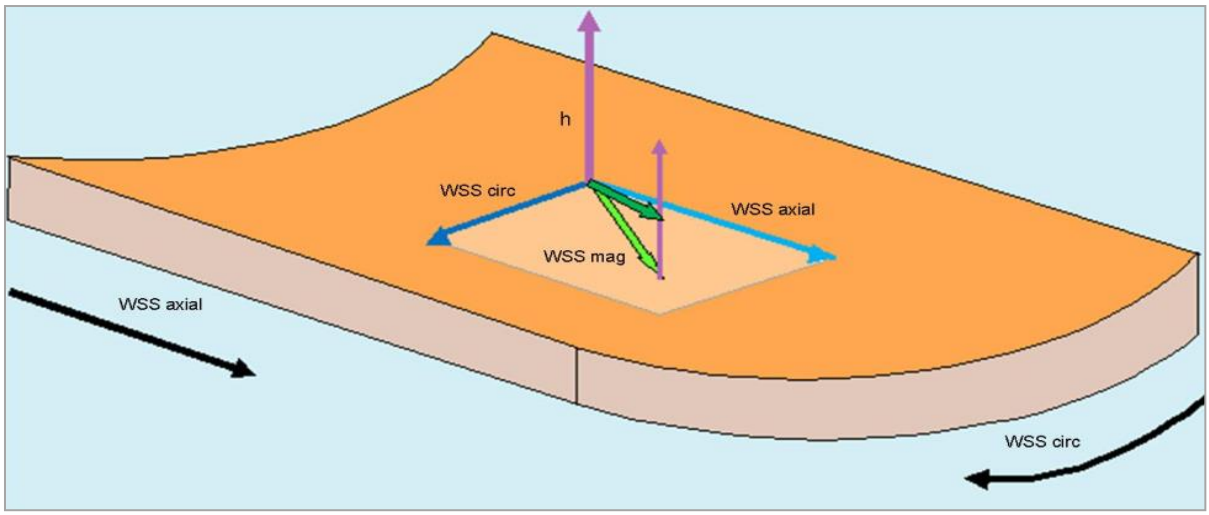

Figure 3: Illustration of a vessel wall segment and acting WSS: schematically depicted are axial and circumferential WSS components (WSS $_{axial}$, WSS $_{circ}$) and the vector of WSS $_{magnitude}$. h = height. Modelled after Stalder (Stalder 2009, page: 73).

The present study was initiated to search for new aspects regarding wall shear stress in the AAo of subjects with BAV. Using 4D CMR quantification tools (next sections) developed by the Department of Medical Physics of the University of Freiburg im Breisgau, Germany, it was practicable to derive estimated shear force metrics at the aortic wall in a study group.

1. 3. 2 Oscillatory Shear Index (OSI)

Knowing that flow in the human arteries is pulsatile means that both anterograde and retrograde flow may occur. Besides the temporal amplitude during one cardiac cycle it is therefore also necessary to consider the possibly changing direction of blood flow.

Ku et al firstly defined an oscillatory shear index (OSI) in 1983 (Ku et al. 1985, page: 296) according to the temporal amplitude of shear stress. The formulation was later adapted by He and Ku in 1996 (He, Ku 1996, page: 79) extending the equation to a general 3D case, now also taking in account three dimensional blood flow:

$$OSI = \frac{1}{2}\left(1 - \frac{\left| \int_0^T \vec{\tau} \cdot \Delta t \right|}{\int_0^T \left| \vec{\tau} \right| \Delta t}\right) \qquad (1.5)$$

Where T is the duration of the cardiac cycle, τ is the instantaneous WSS vector and t time.

OSI data were routinely acquired during quantification. However, it played a minor role in this work.

1. 4 Four-Dimensional Cardiovascular Magnetic Resonance

Basing on latest approaches in four-dimensional cardiovascular magnetic resonance (4D CMR) this work only was possible to perform. This section describes 4D CMR as a diagnostic tool and provides an overview of basic CMR principles fundamental for the 4D CMR sequences having been used.

1. 4. 1 CMR as Routine Diagnostic Tool

CMR is a non-invasive diagnostic tool offering uniformly high image quality in multiple planes, good spatial resolution as well as excellent contrast between blood and cardiovascular structures (Dinsmore et al. 1986:, page: 312). After first reports about cardiovascular applications of magnetic resonance in the 1980s (McNamara, Higgins 1984, page: 167; Herfkens et al. 1983, abstract), in 2006 CMR has been declared to be an appropriate tool for the evaluation of ventricular and valve function, specially "assessment of complex congenital heart disease including anomalies of coronary circulation, great vessels, and cardiac chambers and valves" (Appropriateness of CCT and CMR, 2006, page: 1486, table 16).

Among non-invasive imaging also computer tomography (CT) provides excellent spatial and contrast resolution. However, cardiac CT exposes the patient to high dose ionizing radiation which should specifically be avoided in paediatric cardiology (Higgins et al. 1984, page: 666). Besides CMR and CT also echocardiography, a fast and inexpensive tool with high spatial-temporal resolution, permits to obtain diagnostically high valuable images, particularly of heart valve structure (Higgins et al. 1984, page: 666) and will remain a main column in clinical cardiac diagnostics (Wood 2006, page: 595). Still, aortic imaging by echocardiography can be hampered due to higher operator dependency (Amano et al. 2010, page: 1483) and reduced image quality by bone and air transmission especially in older children and adults (Dinsmore et al. 1986, page: 312).

Despite high costs, the lack of availability of CMR equipment and its often only complementary diagnostic function to echocardiography CMR has become a very important tool in assessing congenital heart disease, like CoA (Schlesinger, Hernandez 1996, page: 140; Wood 2006, page: 606), and is even ranked as "gold standard for aortic imaging" (Myerson 2007, page: 3). CMR also is part of daily routine for evaluating haemodynamic issues like functional analysis or volumetric measurements (Rebergen et al. 1993, page: 1452; Wood 2006, page: 600).

Moreover, during the last ten years CMR has been shown to be a sufficient method for comprehensive in vivo flow and flow force quantification, like 3D flow fields and wall shear stress values (Stalder et al. 2008, page: 1219). These latest applications making possible to acquire 4D CMR

data may yet not be involved in clinical routine but already contribute to understand complex haemodynamic circumstances in different cardiovascular pathologies (Bammer et al. 2007, page: 137; Markl et al. 2011, pages: 18-19).

1. 4. 2 CMR Basics

Nuclear magnetic resonance, and its application in cardiology, cardiovascular magnetic resonance (CMR), is a sophisticated phenomenon which to comprehensively describe requires complex knowledge of quantum mechanics and statistical physics. The author confines to only draw a theoretical picture of basic principles in flow sensitive CMR, e.g. hardware, signal information, imaging and velocity encoding. Please find more exact information in (Ridgway 2010, pages: 4-41; Stalder 2009, pages: 24-39).

CMR systems comprising a main magnet, gradient coils and receiver coils, allow for generating magnetic fields and excitation of certain protons (mostly used in CMR is the hydrogen proton, ^{1}H, due to its abundance in human tissues) into a spinning status by applying a radio frequency pulse (Stalder 2009, pages: 26-27).

The main magnet generates a homogeneous linear magnetic field. Thereby the majority of ^{1}H protons inside of this field align in a coherent shape along a desired vector direction. Alignment of those excited spins causes a net magnetization. This magnetization may be measured. (Simon 2010, page: 25).

By applying high radio frequency impulses spin orientation may be altered and rotated out of the original longitudinal fashion into a status of precession. Duration and strength of those pulses impact the degree of angle of spin rotation in a three dimensional space. This angle is referred to as flip angle and the chosen pulse frequency is named Larmor frequency (Stalder 2009, pages: 29-31).

The transversal magnetization of pre-cessing spins is a voltage inducing process, called phasing, which also may be measured by the prior mentioned receiver coils. Alignment of spinning protons must be seen as an artificial moment. After exposing the spins to the radiofrequency pulse they immediately begin turning back to their original orientation, a process referred to as de-phasing or relaxation which is practically a decay of induced energy. Also relaxation can be measured. Relaxation occurs in two different kinds, T1 and T2. T1 relaxation describes the process of spin de-phasing to their longitudinal shape in the main magnetic field. T2 de-phasing covers the decay of

energy due to spin-spin interaction, as every spin may influence the neighbouring spin, as well as due to static field inhomogeneity (Ridgway 2010, pages: 10-12).

Relaxation time differs amongst tissues, depending on the quantity and quality of ^{1}H-protons, e.g. if they are free or bound. The measured relaxation can be transformed into images leading to image contrasts between tissues depending on their relaxation times (Simon 2010, page: 26).

After applying the radio frequency pulse, three gradient coils allow for generating a superimposed linear magnetic field gradient on the static magnetic field to localize the spatial origin of a signal. This gradient can be applied three dimensionally (3D). This way, each spinning proton rotates at a different frequency along the gradient. According to their relative position their frequency is either decreased or increased by the gradient. This procedure called phase encoding allows for exact signal localizing of different spins. To derive 3D image data information measurement must be performed successively with different magnetic field gradients in three dimensions (Ridgway 2010, page: 19).

The frequency encoded signal may be transformed with a mathematical tool called Fourier transformation. Splitting the frequency signal into single components, each component has got its own frequency amplitude along the gradient. Thus, all amplitudes may be mapped onto a location (Ridgway 2010, page: 19).

Finally, one may tell the CMR signal is proportional to the number of excessed spins and thus a frequency description of spin density leading to image contrasts between tissues depending on their signal intensity (Stalder 2009, page: 33). Gradient coils help to detect the location of a signal.

Radiofrequency pulses and gradient strength can be switched on and off in a fixed order and in numerous variations regarding frequency and strength, depending on the aim of imaging, e.g. only morphological structures for orientation (“localizer” sequences) or more comprehensive 3D T1-weighted imaging of the aorta like in the present study, described in the study protocol in section 2.

Images of the beating heart can be obtained using CINE imaging. This method requires data acquisition at multiple time points during the cardiac cycle to compose one complete image. Data are obtained during several cardiac phases synchronized using ECG to always capture data at the same time frame and in the same anatomic position for each heartbeat. Interleaving parts minimize movement confounders of the heart (R wave of systole). This way, a separate image of each cardiac phase can be generated. Ordering those enables to view them as a movie sequence, often just named CINE. (Ridgway 2010, page: 36).

1. 4. 3 Image Quality Improving CMR Applications

CMR is naturally hampered by moving artefacts as the heart is a moving organ and additionally due to breathing movements.

ECG triggering minimizes artefacts in CMR by measuring only within a heart rate synchronized acquisition window. Trigger moment would be the R wave of the cardiac cycle and measurement is mostly performed during diastole when heart or aorta move least. However, ECG trigger increases study duration and is not possible to perform in presence of arrhythmia (Ridgway 2010, pages: 36-37)

Breathing is the second major moving confounder. One method to reduce that is breath-holding. As breath-holding is only possible for approximately 30-45 sec, the resulting scan time is very short. This increases signal to noise ratio and reduces image quality (Simon 2010, pages: 28-29). Another solution would be navigated “gating windows” where a navigator registers the motions at the liver-lung border. This tool enables to detect moments of lowest breath movements during which measuring may then be performed. Even though, scan time is increased by this application, imaging quality is clearly improved (Markl et al. 2007, page: 830).

Both ECG triggering and navigated breathing window technique were applied in this work.

1. 4. 4 Flow-Sensitive CMR

Also flow-sensitive examinations may be performed with CMR. Basing on the principle that the magnetic signal of moving objects inside of a gradient field contains an additional phase, subtracting this velocity encoding phase image from a reference image permits quantitative measurement of moving tissue or blood flow. The operator has to adjust an estimated “venc” (velocity encoding) for CMR measuring to avoid velocity artefacts and reduce signal to noise ratio in phase images. This imaging scheme is referred to as phase contrast CMR (PC CMR). (Unterhinninghofen et al. 2007, page: 1012).

Connecting PC CMR with the CINE technique blood velocities can be measured time-resolved and presented as movies throughout the cardiac cycle (Simon 2010, page: 31). To obtain 2D velocity data with this procedure belongs to daily routine in CMR. Improvements in information technologies during the last decade have created the possibility to extend this procedure to all three spatial dimensions. Thus, today it is technically possible to derive three directional, time-resolved and three

dimensional velocity and flow data (4D). This requires time as every instant of the entire cardiac cycle must be measured four times (reference image, three dimensions of velocity). Assuming a periodic heart beat the sequences may be applied over many heart cycles to obtain data for all segments of one heart phase. Joining them in the end allows for 4D velocity and flow measuring.

Together with ECG triggering and navigator supported dynamic breath gating improved by Markl et al (Markl et al. 2007, page: 830) it is practically realizable to obtain three dimensional flow and velocity mapping with minor moving artefacts over the time of one assumed heart cycle.

Aiming to find new insights into wall shear stress in the AAo of individuals with BAV, 4D CMR with its latest features as the ideal diagnostic tool was used for the presented study.

2 Patients and Methods

2. 1 Patient and Control Group

This section spans a description of both patient and control group (sections 2.1, 2.2), including a list of criteria for inclusion or exclusion and a table of demographical data.

2. 1. 1 Patient Group

Search for patients with known BAV was done using the database of German Heart Centre Munich, Technische Universität München (TUM). Flowchart in *figure 4* provides an overview. Criteria of inclusion and exclusion are listed in *table 1*. The next sections describe the design process.

Criteria	Subcriteria	Inclusion	Exclusion	Other reasons leading to Exclusion
Age	≥ 8 years	x		Arrhytmia
Bicuspid aortic valve (BAV)		x		Prior cardiac surgery
Aortic regurgitation	mild (< 30 % RF)	x		Heart failure
	moderate or severe		x	Cardiomyopathy
Aortic stenosis	mild (< 25 mmHG)	x		Myocarditis or endocarditis
	moderate or severe		x	Arterial or pulmonary hypertension
Jet velocity above valve	≤ 250 cm/sec	x		Pregnancy
	> 250 cm/sec		x	Claustrophobia or metal implants
Velocity gradient in the descending aorta	> 250 cm/sec		x	Marfan's syndrome, other connective tissue defects
Aortic diameter	≤ 45 mm	x		Coarctation of the aorta
	> 45 mm		x	Any other cardiovascular malformation
Mitral valve prolapse		x		Pectus excavatum
Persistent foramen ovale		x		Down syndrom, mental impairment, others
Pulmonaray artery stenosis	mild	x		Antihypertensive drugs, oral anticoagulation
	moderate or severe		x	Contraception with intrauterine metal device

Table 1: Criteria of Inclusion and Exclusion; Classification of aortic regurgitation, aortic stenosis, aortic dilation and velocity gradient according to the guidelines of the American heart association (AHA) (Bonow et al. 2008, page: e536); RF = regurgitation fraction.

Initially, data base with about 32000 patients was searched for appropriate subjects, starting in August 2008. Terms having been looked for were the words ‘Bicuspid’ and ‘Bikuspid’. Originally, 989 of circa 32000 patients with the diagnosis of BAV could be detected, checking the past 20 years, retrospectively. Their files were systematically reviewed for exact diagnosis, *figure 4*.

This way, 636 subjects had to be immediately excluded as they did not meet the inclusion criteria (*table 1*). Twelve of the 636 patients were incorrectly listed among the results, actually having TAV. The remaining 624 individuals did either show one or more exclusion criteria (*table 1*) or, during

second review process, were assessed to be inadequate due to increased echocardiographically measured values of aortic regurgitation fraction (RF) or aortic velocity gradients.

Then, 353 patients with BAV meeting the inclusion criteria were still listed. Unfortunately, contact data (phone number, address) were available in only 98 cases. Secondly, contact process was started in September 2008. The strategy having been followed intended to contact individuals by phone to personally inform them about the study.

Subjects were contacted according their life place, starting with patients based in Munich, successively proceeding to those living in the surrounding area of Munich and later all persons resided farther away (n = 76 of 98). In 28 of these cases (n = 28 of 76) phone number was incorrect. These persons were subsequently tried to reach via mail, if address data were known (n = 11 of 28).

When no phone number was available on contact details (n = 22 of 98), subjects were directly contacted via mail, informed about the study and asked to write or call back.

Together, 33 individuals received information via mail (n = 33 of 98). Merely a minority from these 33 replied on the postal approach and could then be called (n = 3).

Thus, all together only 51 could be phoned, 48 directly and 3 after mailing contact. Of those 51 persons having being called 15 refused participation in the study.

In case of interest (n = 36) to attend the study, medical history of patient was asked, especially current medication, diseases or syndromes not meeting the inclusion criteria, such as hypertension or claustrophobia; also metal implants were asked for. Additionally, women were questioned for pregnancy. Complete exclusion criteria are listed in *table 1*. When patient was uncertain about required data, in some cases the patient's family doctor or medical specialist had to get in touch with to receive further information about the current medical status of the patient, specifically concerning cardiac diagnoses. This happened, without exception, in accordance with the patient.

Within another 11 candidates had to be excluded; four reported to actually have TAV (n = 4) and seven did not meet the inclusion criteria, as for diagnosis of trisomy 21 (n = 1), anti-hypertensive medication (n = 4) or increased velocity gradients in the aorta (n = 2).

Subjects who fulfilled the required inclusion criteria (n = 25) was sent additional, written information material about the study. Afterwards, patients were called again on a fixed date. When the patient still agreed with the terms of study an examination date was arranged (n = 25).

Finally, in step 3 of patient group acquisition, 25 patients (n = 25) were invited to undergo 4D CMR at the Department of Radiology, at German Heart Centre Munich, TUM. Between December 2008 and

May 2009, while carrying out step 3, one more patient (n = 1) with BAV receiving routine check-up at the out-patient clinic of the Department of Paediatric Cardiology and Congenital Heart Disease, at German Heart Centre Munich, TUM, could be added to the study group.

All 26 study subjects underwent 4D CMR examination (n = 26). Afterwards, eight more subjects had to be excluded (n = 8) for different reasons, such as aortic dilation larger than 4.5 cm in the AAo (n = 2), previously unknown arterial HTN (n = 1) and one for the reason of flow velocities higher than 2.5 m/sec, measured above the aortic valve (n =1). Among the remaining four measurement error occurred and data were not usable (n = 4).

In the end, 18 subjects with BAV and no concomitant vessel disease, having undergone flow sensitive CMR formed the study group (n = 18) which could then be opposed to an age and sex matched control group (next section). Demographical data together with basic medical values (P_{sys}, P_{dias}, BSA) of the study and control group are listed in *table 2*.

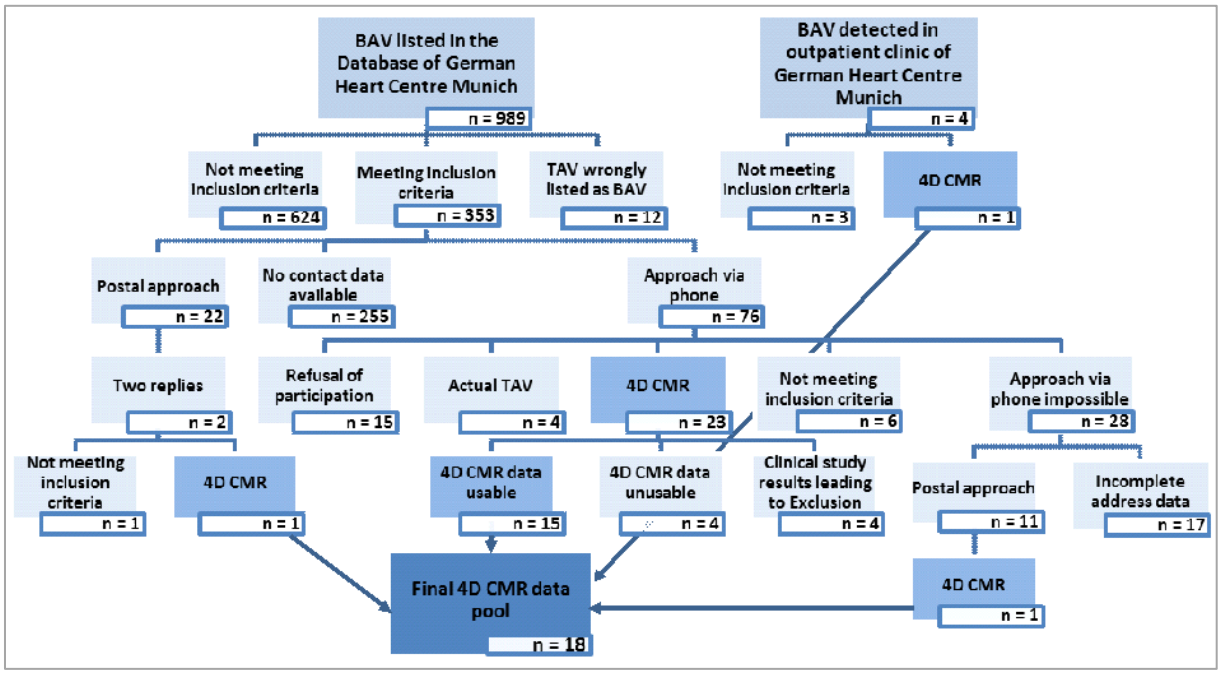

Figure 4: Flowchart of study group design

2. 1. 2 Control Group

The age and sex matched control group of 18 healthy individuals (n = 18) with native TAV was formed after the study group had been designed. Inclusion and exclusion criteria were the same as for the patient group mentioned above (*table 1*). Recruitment was performed via announcements amongst staff at German Heart Centre Munich, TUM. Demographics of the control group are listed in *table 2*.

Demographical data of control and patient population					
Criteria		**Controls with TAV**		**Patients with BAV**	
		n = 18		**n = 18**	
		mean	**SD**	**mean**	**SD**
Age	yrs	26.1	± 8.0	26.20	± 8.4
Height	cm	174	± 13.8	175	± 12.1
Weight	kg	68.1	± 16.4	68.9	± 14.9
BSA	[m²]	1.8	± 0.3	1.80	± 0.2
P_{sys}	[mmHg]	107.1	± 7.7	110.9	± 9.6
P_{dia}	[mmHg]	59.7	± 11.2	65.7	± 11.6
Dmax corrected	[cm/m²]				
Bulbus aortae		1.62	± 0.23	1.76	± 0.24
Ascending aorta		1.57	± 0.2	1.89	± 0.26
Descending aorta		1.08	± 0.11	1.05	± 0.17

Table 2: Demographical data of study and control population including mean values and standard deviation (SD); BAV = bicuspid aortic valve; BSA = body surface area; P sys = systolic blood pressure; P dia = diastolic blood pressure; Dmax corrected = maximum diameter normalized to BSA (Roman et al. 1989, page: 510).

2. 2 Methods

Values are presented as mean ± standard deviation. Literature was obtained by online search on pubmed.org, google.com, at the Bavarian State Library and from personal correspondence with paediatric cardiologists and associate professors at German Heart Centre Munich, TUM.

2. 2. 1 Study Conditions

The presented study was initiated by the Department of CMR for Paediatric Cardiology and Congenital Heart Disease at German Heart Centre Munich, University hospital of Technische Universität München, TUM. It was designed prospectively. Written approval by the ethics committee of TUM was given.

All participants, patients and control group, were informed by written and oral explanation about the study, the study conditions and the procedure. All participants gave their written consent. No subject received financial support.

Examinations were performed under clinical conditions at our hospital, German Heart Centre Munich. At least one paediatric CMR specialist assisted by a technician or a medical student was present during the entire procedure. All examinations were performed without anaesthesia while patient was totally conscious. Electrocardiogram (ECG) and blood pressure (P_{blood}) were continuously monitored with MR-compatible monitoring systems. Headphones were placed to minimize noise disturbance. The mean study time was approximately 40 min. No contrast material was applied.

Per definition the aorta was segmented into ascending aorta (AAo), aortic arch, and descending aorta (DAo) as depicted in *figure 5*. WSS measurement was performed in the middle and distal ascending aorta. X axis of supporting coordinate system was directed to the ventral vessel wall also referred to as outer curvature of the aorta. Y axis always was positioned left-hand side.

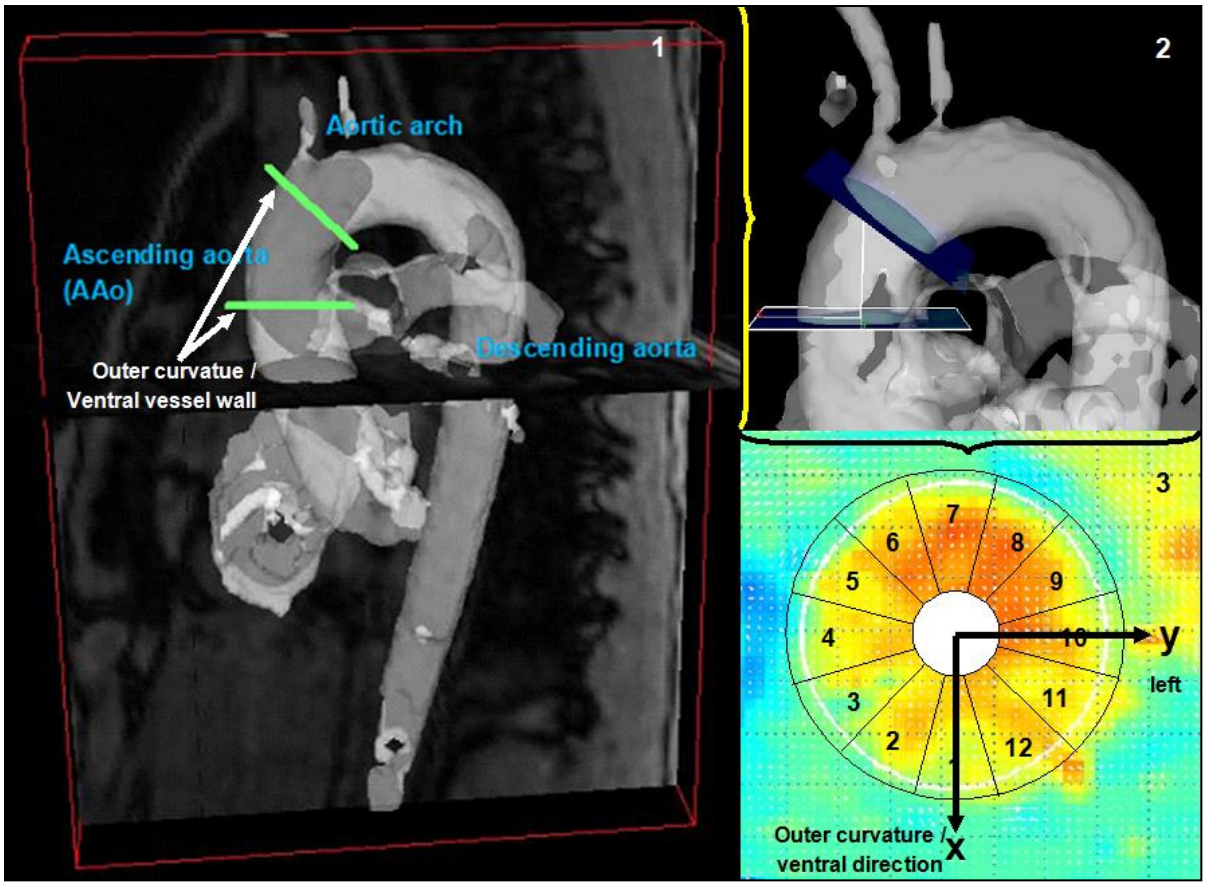

Figure 5, *panel 1*: Definition of anatomic terms, landmarks of WSS estimation (green baulks) in a 3-D isosurface of the thoracic aorta; *panel 2:* supporting coordinate system in 3D vessel animation at level of the ascending aorta, zoom; *panel 3*: orientation of coordinate system with X and Y axis and vessel wall segmentation into 12 sub-segments, view from below; screen shots of EnSight© (ENSIGHT ©, by CEI, Apex, NC, USA) and "flow_tool" user surface.

2. 2. 2 4D CMR Data Acquisition and Processing

2. 2. 2. 1 Acquisition Protocol

CMR was performed with a 1.5 Tesla Siemens Magnetom Avanto, Siemens, Erlangen, Deutschland, at our hospital, German Heart Centre Munich, at the Institute of Radiology.

At first, planning sequences, referred to as localizer in three orthogonal slices were obtained for registration of the thoracic anatomy. Secondly, straight axial CINE imaging of the aortic valve was performed to prove bicuspid or tricuspid aortic valve structure, regarding to (Schaefer et al. 2007, page: 687). Depending on the evaluation the examined individual was finally referred to BAV or TAV group. For unclear evaluation the protocol intended for exclusion of the examined subject from the study. This case never occurred.

Following, CINE imaging of the thoracic aorta was done; the first at the level of Sinus of Valsalva, the second of the middle AAo at the level of the right pulmonary artery, and the third one of DAo at the level of the left pulmonary artery. From the obtained images aortic diameter could be measured (*table 4, results*).

Also velocity gradients in the aorta were estimated. With regard to the gradient "venc" (velocity encoding) was adjusted. Highest chosen "venc" in this study was 230 cm/sec. An estimated velocity gradient above 250 cm/sec led to exclusion from the study (*table 1*).

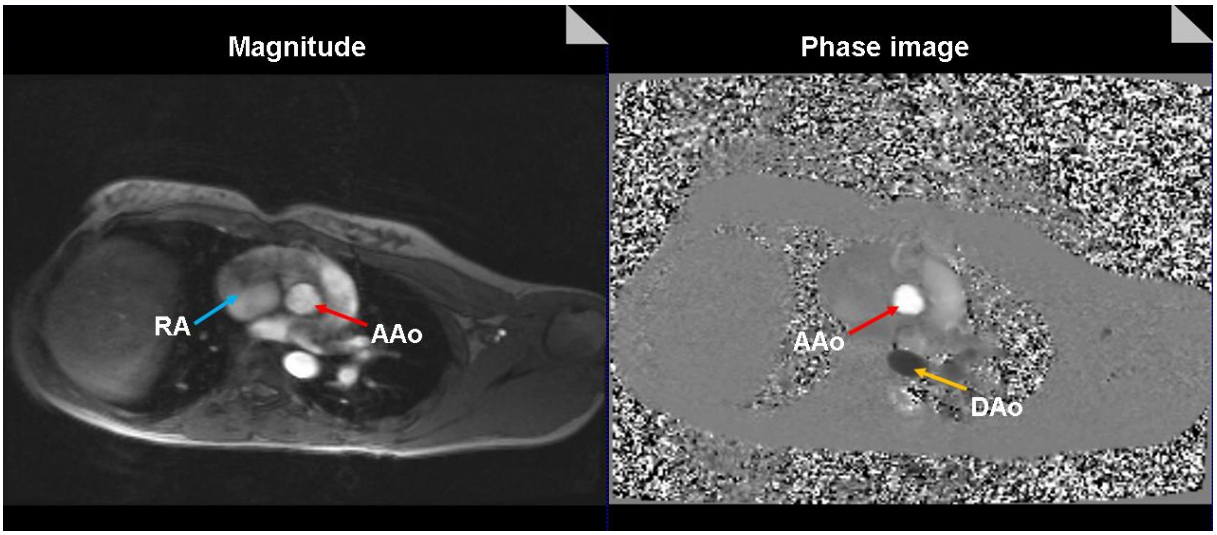

Figure 6: Magnitude and phase image of the ascending aorta (AAo); RA = right atrium, DAo = descending aorta. Phase contrast image: white flow direted to the head (AAo), dark flow caudal (DAo). Data from a 25-year old volunteer. "Argus" screenshots, Siemens. CMR by Siemens "Avanto" 1.5 T; Siemens, Erlangen, Deutschland.

Finally, aortic blood flow was imaged using a time-resolving 3-dimensional phase contrast sequence with three-directional velocity encoding. The sequence was used with the permission of Michael Markl, PhD, University of Freiburg im Breisgau, Germany. ECG triggering in connection with navigated respiratory gating whilst free patient breathing, were applied. (Stalder 2009, pages: 57-61). Study time was approximately 20 up to 40 minutes according to the heart rate, whereat subjects with slow heart beat had a longer examination time.

Acquisition parameters are listed in *table 3* and were performed according to Markl et al.

Study protocol			
Sequence	3D gradient echo sequenz with 3 directional velocity encoding	**Routine**	
Dimension	3D	Field of view	240 x 320 mm
Velocity encoding	Vx, Vy, Vz	Field of view phase	75%
In-plane venc	200 cm/sec	Layer thickness	2.5 mm
Trough-plane venc	200 cm/sec	Repetition time TR	39.2 msec
	230 cm/sec according to aortic jet (only once)	Time to echo TE	2.417 msec
Echo- spacing	4.9 msec	**Resolution**	
MR system	1.5 Tesla Magnetom Avanto, Siemens, Erlangen	Spatial resolution	2.1 x 1.7 x 2.5
Bandwidth	460 Hz/Px	Base resolution	192
Physio		Phase resolution	81%
ECG trigger	prospective	Slice resolution	75%
Respiratory gating	applied	**Contrast**	
Contrast material	no	Flip angle	8 degrees

Table 3: 4D CMR acquisition protocol, according to Markl et al, University of Freiburg, Freiburg im Breisgau, Germany; ECG = electrocardiogram, venc = velocity encoding.

Figure 7 depicts acquired flow-sensitive time-resolved CMR information. As previously described a magnitude reference image was obtained before velocity and flow data in three dimensions were generated over time. Automatic linking of images in chronological order allowed to design CINE movies of one heart beat including ejected flow throughout the aorta.

2. 2. 2. 2 Data Conversion

After having performed 4D CMR the acquired data were exported to CD-Rom. Later they were read into a special software tool named “Copy tool” (based on MATLAB; The MathWorks, Natick, MA, USA) designed by the Department of Medical Physics, University of Freiburg. Software was used with kind permission of the University of Freiburg.

“Copy tool” supports DICOM (digital images and communication in medicine) data, to convert and to compatible images for pre-processing. Moreover, the tool selects flow-sensitive data from magnitude images. Different folders for each kind of image file were created.

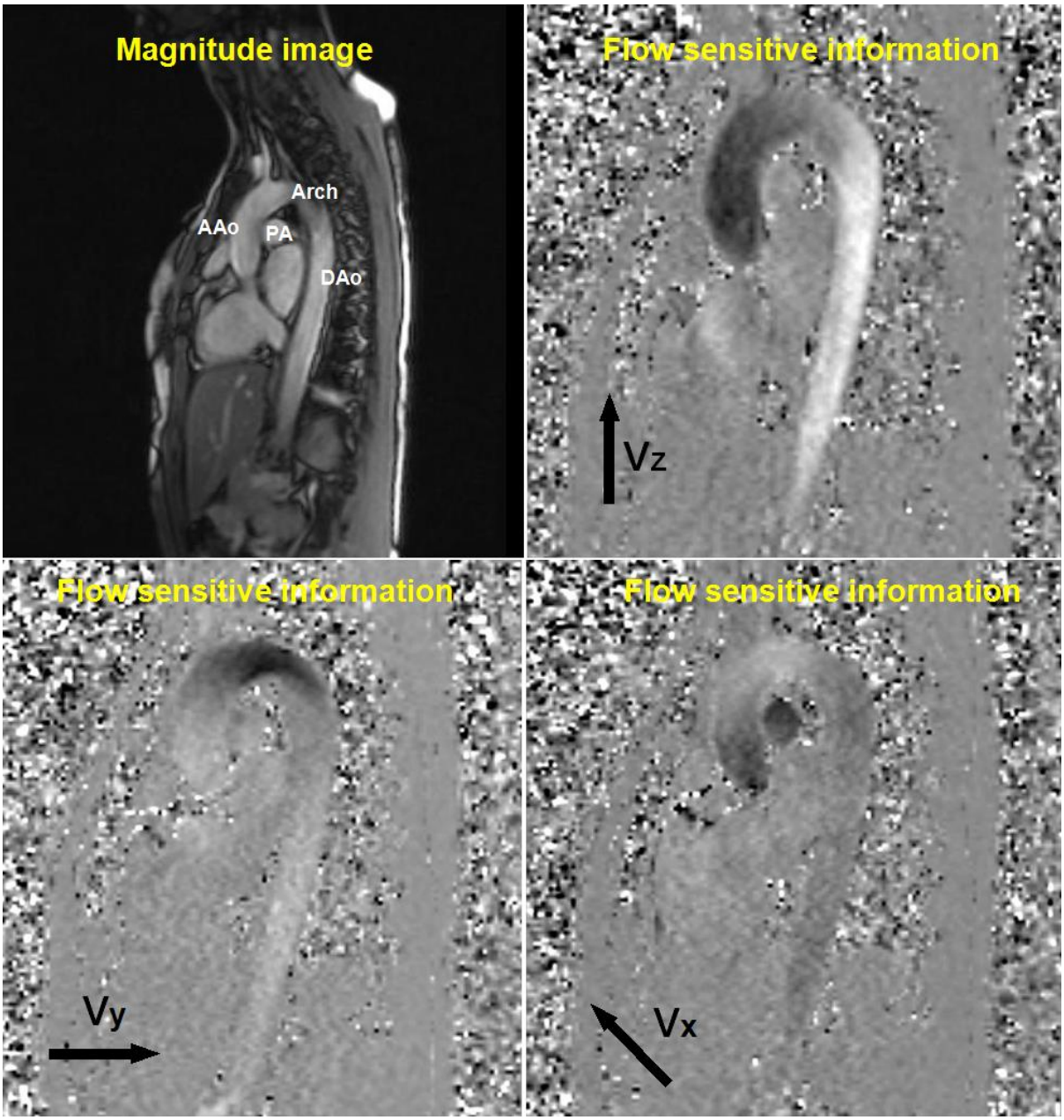

Figure 7: Flow sensitive CMR: magnitude reference image (panel top left) and flow sensitive data for all three spatial dimensions. V = velocity, AAo = ascending aorta, DAo = descending aorta, PA = pulmonary artery. Data derived from a 25-year old volunteer. 4D CMR by Siemens "Avanto", 1.5 T. Siemens, Erlangen, Deutschland.

2. 2. 2. 3 Pre-processing

Copied magnitude image data could then be input to "Velomap", designed by the Department of Medical Physics, University of Freiburg im Breisgau, Germany.

During 4D CMR certain errors may occur and affect imaging. Such artefacts were measurement noise, eddy currents, or aliasing. Eddy currents are induced by rapid switching of magnetic field gradients while CMR. Aliasing may occur when the chosen "Venc" (velocity encoding) during CMR is

lower than the actual velocity. Measurement noise can develop through magnetic field inhomogeneity.

"Velomap" allowed for correction of such errors in phase contrast images (*figure 8*). The goal was to delete all disturbing information without cancelling out aortic blood flow data. To ensure that in all participants, an image slice with best sight on ascending aortic blood flow was chosen (slice 12 of approximately 25 in *figure 8*), time phase was elected during systole (phase 4 in *figure 8*) and spatially-resolved velocity was adjusted to direct coronal (*figure 8*).

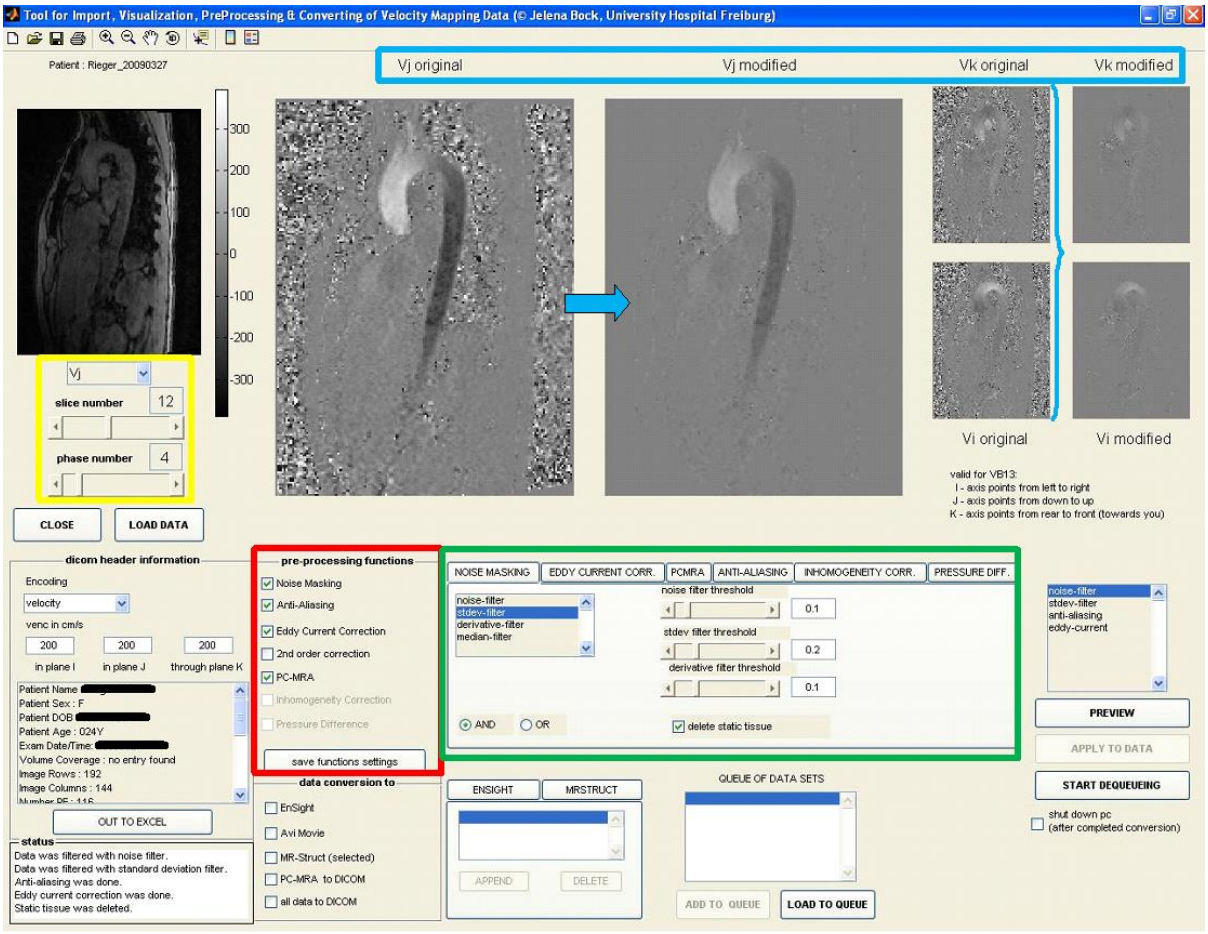

Figure 8: "Velomap" screenshot. Yellow box: options to select one spatial direction of flow sensitive information, velocity image in Z axis ("Vj" = velocity), image slice number ("12"), and cardiac phase ("4", during systole); images in centre top show original and modified version after error correction. Red box displays checked error correction options. Green box shows fine tuning for individual noise filtering. (Stalder et al. 2008, page: 1219; Stalder 2009, page: 61).

Error correction for all individuals of both study and control group was performed in a standardized fashion. The red box in *figure 8* depicts the available error correcting functions. In general chosen were "anti-aliasing", "eddy current correction", "standard deviation noise filtering". "Static tissue" was deleted in all data too. Green box (*figure 8*) displays fine tuning function. This only was used for

observer-based “noise filtering” regarding to image quality and was performed individually in all participants. Note that not all disturbing information was possible to delete (“static tissue”, *figure 9*).

Once pre-processing was accomplished and changes applied, the set data were saved and CMR information converted for the next step.

2. 2. 3 Visualisation of Vessel Structures and Aortic Blood Flow

Pre-processed data were transmit to dedicated post-processing software called EnSight ©, a product by CEI, Apex, NC, USA, *figure 9*.

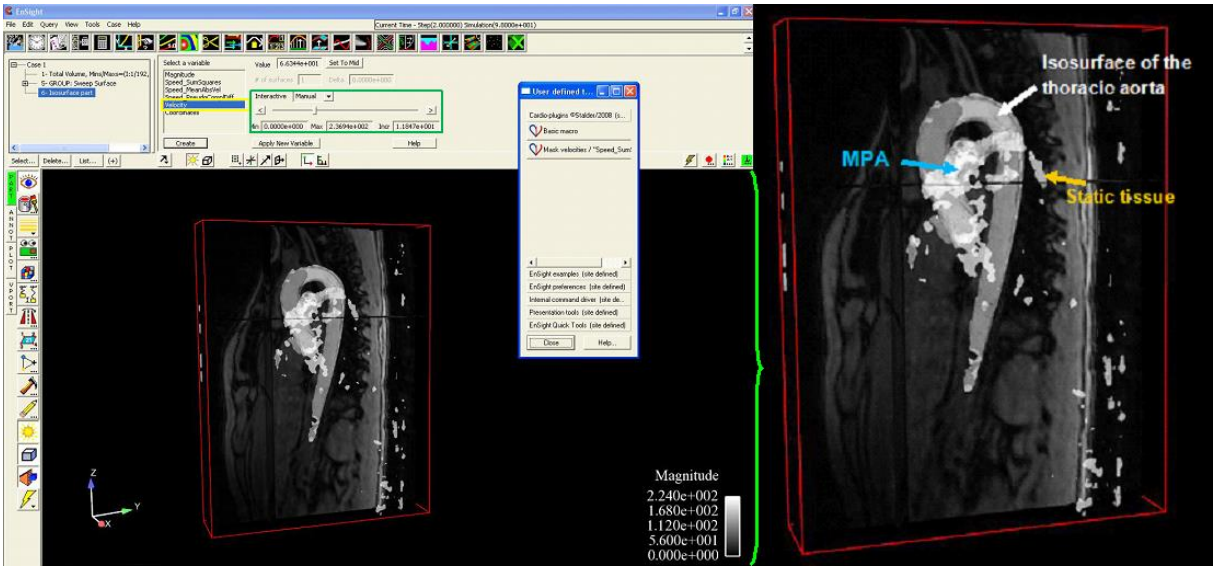

Figure 9: ENSIGHT © screen shot; ENSIGHT © user surface displaying several setting tools on the top row and on the left; centre showing the region of interest with 4D CMR data set. Iso-surface of the thoracic aorta in a 24-year old woman; background magnitude image helped for anatomical orientation; colours are given in absolute values. Yellow box depicts “velocity” as iso-surface parameter. Green box shows threshold adjustment. Right image presents zoomed version with remaining main pulmonary artery (MPA) and static tissue. (ENSIGHT ©, a product by CEI)

ENSIGHT © was used to generate 3D interactive anatomical images of the thoracic aorta as depicted in *figure 9.* Disturbing visualised structures like the main pulmonary artery (MPA), “measuring noise” or static tissue covering the view on the aorta were deleted as far as possible by downsizing the “total volume” (red box in *figure 9*) and setting of threshold values for velocity data (green box in *figure 9).* Minimum threshold of velocity was chosen higher than usually common in veins. This way velocity information besides the aorta could widely be corrected.

Once an ideal sight on the thoracic aorta was found flow-sensitive CMR information was additionally loaded. This allowed for animated 4D flow visualisation and was used to create instantaneous stream lines and time-resolved particle traces of blood flow in the thoracic aorta, *figure 10*.

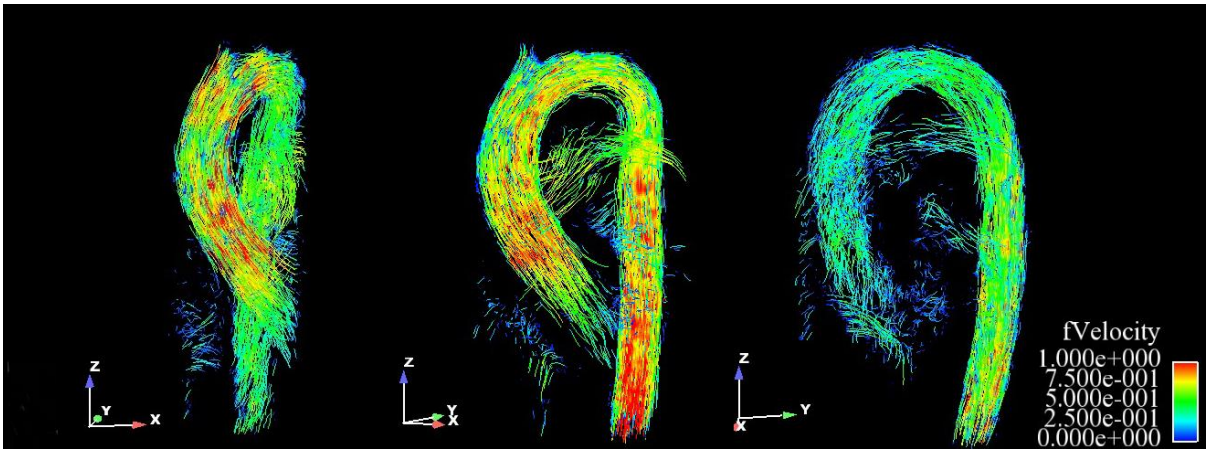

Figure 10: Streamline 4D blood flow visualization of aortic flow in a healthy 27-year old male; left image: ventral view during early systole; centre: ventral-lateral view during mid-systole; right image: lateral view during end systole; V z is sensible for main aortic flow in the ascending and descending aorta, V y presents flow in the aortic arch and V x visualizes blood flow coming out of the heart; corner down right: colour coding = local velocity magnitude. ENSIGHT © screenshots (ENSIGHT ©, by CEI, Apex, NC, USA).

Streamlines may be understood as trajectories which represent measured instantaneous flow vectors forming a 3D impression of blood flow patterns at a certain moment, *figure 10*. Particle traces are a visualising tool to show time-resolved blood flow information over an arbitrary time period, where particles follow the track of measured flow. Particle trace flow may be watched as a movie (Frydrychowicz et al. 2007a, page: 468).

Blood flow was visualised for controlling whether flow sensitive 4D CMR data were adequately imported. In this step, ENSIGHT © served for ideal 3D depicting of the thoracic aorta as well as visualising of 4D aortic blood flow. This also introduced velocity and wall shear quantification process (next section).

2. 2. 4 Wall Shear Stress Data Acquisition and Quantification

2. 2. 4. 1 Data Acquisition with Velocity Encoding 2D Planes

As described in the section before 4D CMR data were applied to ENSIGHT © and could then be used to obtain aortic velocity data and wall shear stress measurements. Velocity data measurement was performed in the middle and distal ascending aorta. Orthogonal square 2D planes were manually positioned along the 4D datasets of the AAo at defined landmarks which were, approximately, the level of the bifurcation of the main pulmonary artery (MPA level, middle AAo) and further downstream in front of the branching brachiocephalic trunk (BCT level, distal AAo), as illustrated in *figures 11 and 12.*

Planes were placed at right angle to the vessel wall (*figure 11, panel 1*), transacting the entire vessel, supported by a reference coordinate system with three axes, X, Y and Z. By definition the X axis was aligned ventrally and Y axis in the direction of the left vessel wall (view from below). Z axis was chosen to be parallel to the direction of blood flow (*figure 11 and 12*, *panels c, d and e*).

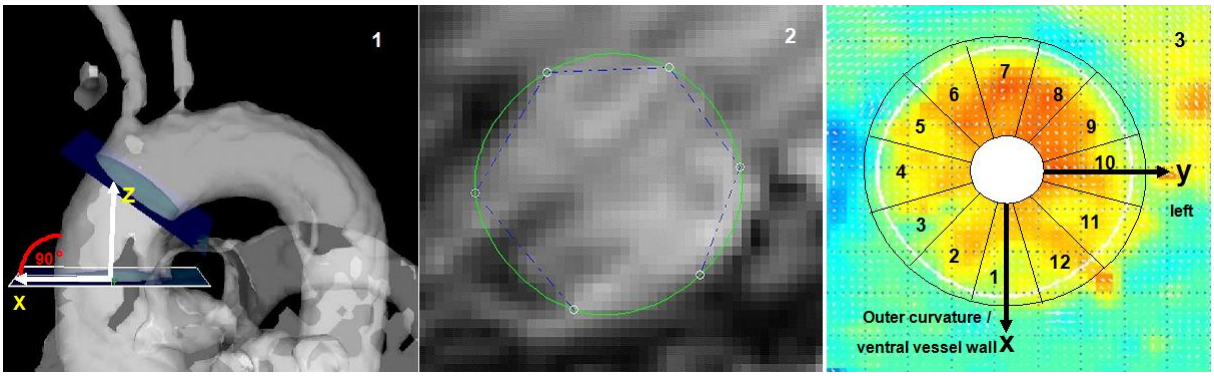

Figure 11: 2D velocity data acquisition in the AAo : *panel 1*) Landmarks for WSS measurement in AAo; planes were placed at right angle. X axis ventrally orientated, Z axis in the direction of flow; *panel 2*) 2D magnitude image of the middle ascending aorta; *panel 3*) 2D velocity profile of the middle ascending aorta with orientation assistance. Screenshots of EnSight © and "flow_tool" usersurface.

Those planes permitted to obtain 3D velocity data in the entire vessel and at the aortic wall. Data were generated at described anatomical spots in the middle and distal AAo. Once planes had been positioned the derived data were saved as "flat files" (ASC II files) and exported. "Flat files" encode for 4D CMR data (section 2.2.4) as well as 2D planar information of velocity and vessel wall parameters (this section). Those generated data were obligate for the next step of quantification (next section), where they were implemented to dedicated quantification software, "flow_tool" (designed by the Department of Medical Physics, University of Freiburg im Breisgau, Germany).

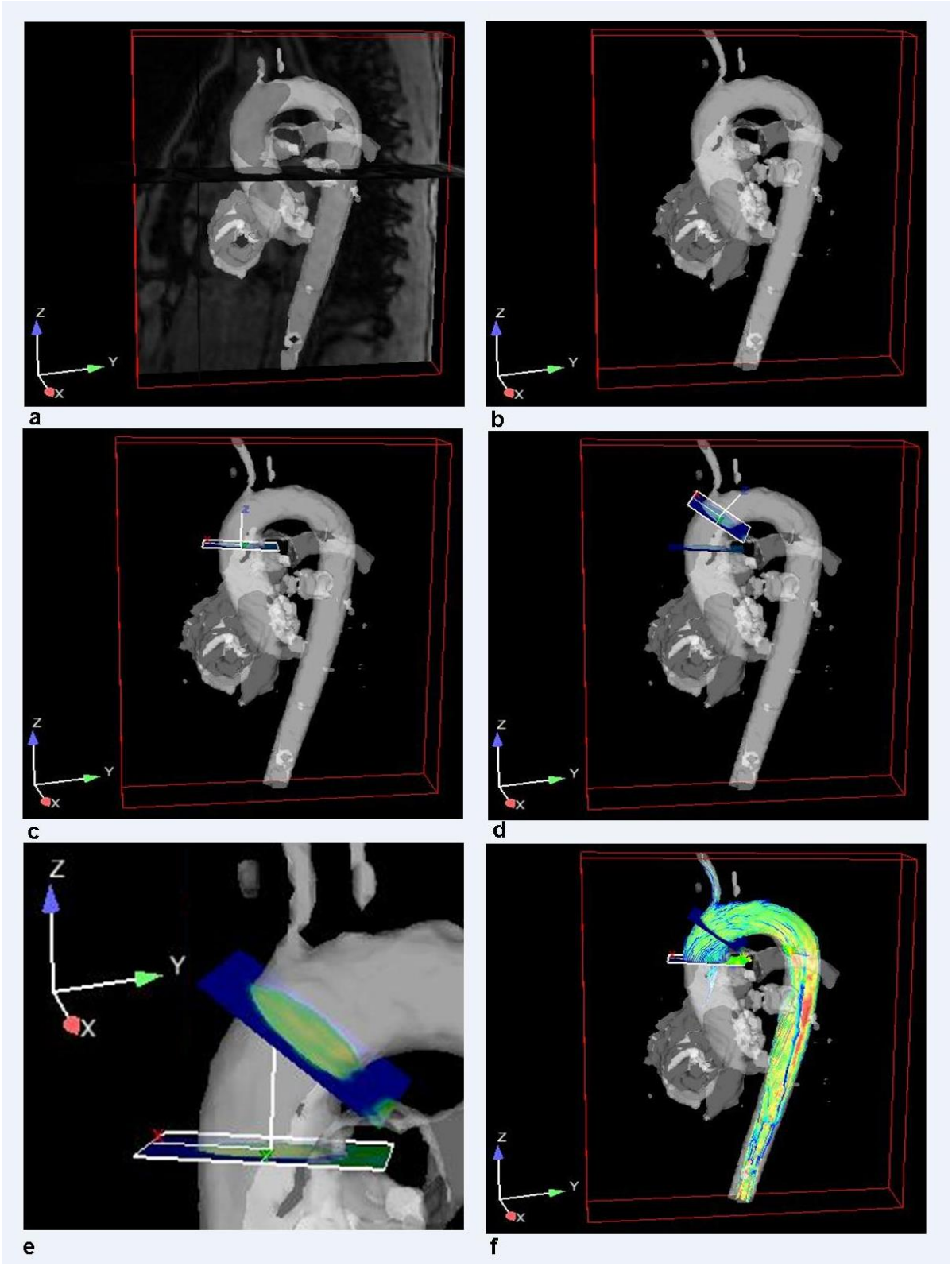

Figure 12: Workflow of plane positioning, ENSIGHT © screen shots: a) Total volume visualisation of a 4D CMR data set of the thoracic aorta in a 25-year old healthy woman; magnitude image applied for anatomical orientation. b) Complete 4D volume without magnitude image. c) First square plane manually placed at right angle (middle AAo) d) Second 2D plane positioned in the distal AAo. e) Zoom of both 2D planes in the AAo. f) Streamlines emitted from mid AAo 2D plane. X axis in ventral direction, Y axis in the direction of left wall and Z axis parallel to the direction of blood flow. Reference coordinate system depicted down left in all six images. (ENSIGHT ©, by CEI, Apex, NC, USA).

2. 2. 4. 2 Data Quantification by “Flow_tool”

“Flow_tool” is software developed by the Department of Medical Physics, at the University of Freiburg, Germany (based on MATLAB (The MathWorks, Natick, MA, USA)). The software was used with permission of University of Freiburg im Breisgau, Germany.

Basically, “flow_tool” allowed for calculation of estimated spatial-temporally resolved velocity and wall shear values. The software computed those by combining 4D CMR information with 2D planar velocity and vessel wall data generated using ENSIGHT© (last sections), (Stalder 2009, pages: 78, 144). Encoded as “flat files” 4D CMR data together with ENISGHT© data sets of 3D velocity encoding planes (section 2.2.5.1) were imported into “flow_tool”, *figure 13.*

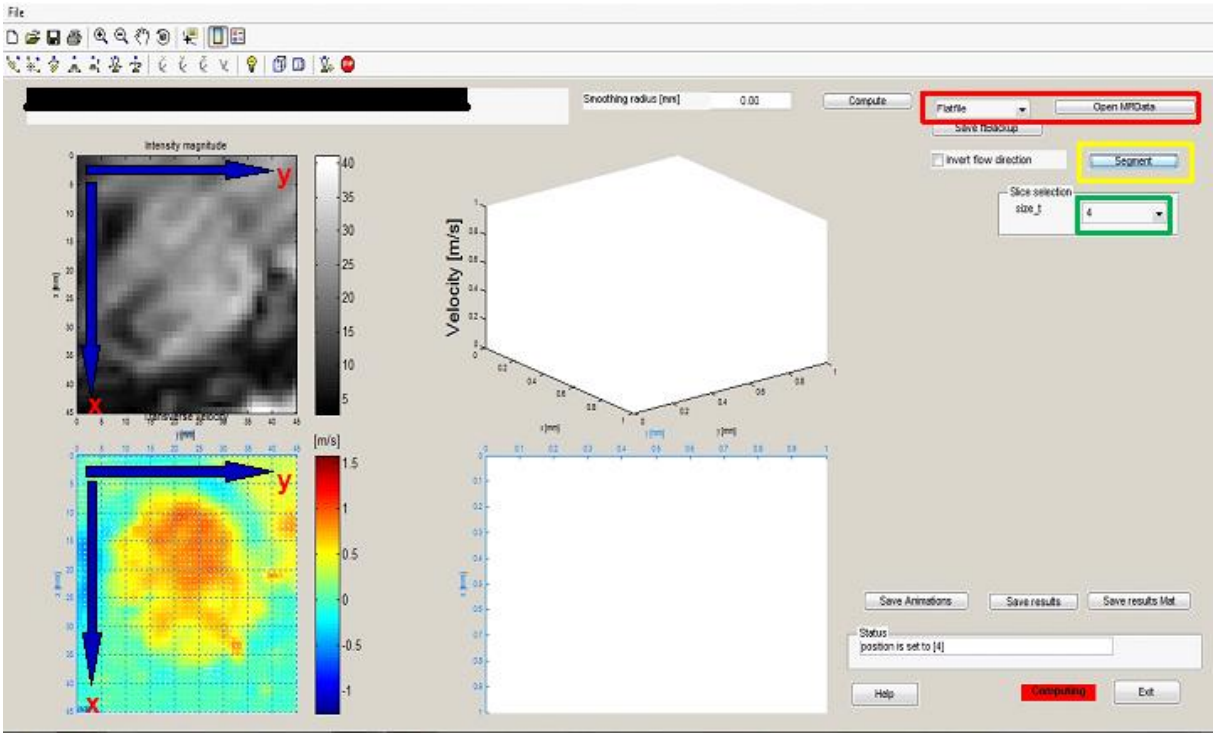

Figure 13: “Flow_tool” user surface: “flat file” upload function of 2D plane ENSIGHT© data (red box); 2D plane velocity data with magnitude image (up left) and 2D velocity profile (down left) during systole; time frame chosen approximately at peak systole, phase 4 of 23 (green box), of cardiac cycle. X axis aligned into direction of the ventral vessel wall of the aorta, Y axis to the left side, view from below. “Segment”-option for region of interest (ROI) tool (yellow box). Velocity profile of a 40-year old healthy male volunteer at level of middle AAo. Screenshot of ‘flow_tool’ usersurface.

An integrated segmentation tool (“ROI tool”, designed by the department of Medical Physics, University of Freiburg im Breisgau, Germany) allowed for observer based segmentation of the region of interest (ROI), *figure: 14*, to define vessel area and vessel wall. Once ROI was fully defined for each time step throughout the cardiac cycle the acquired data were completely processed for final quantification.

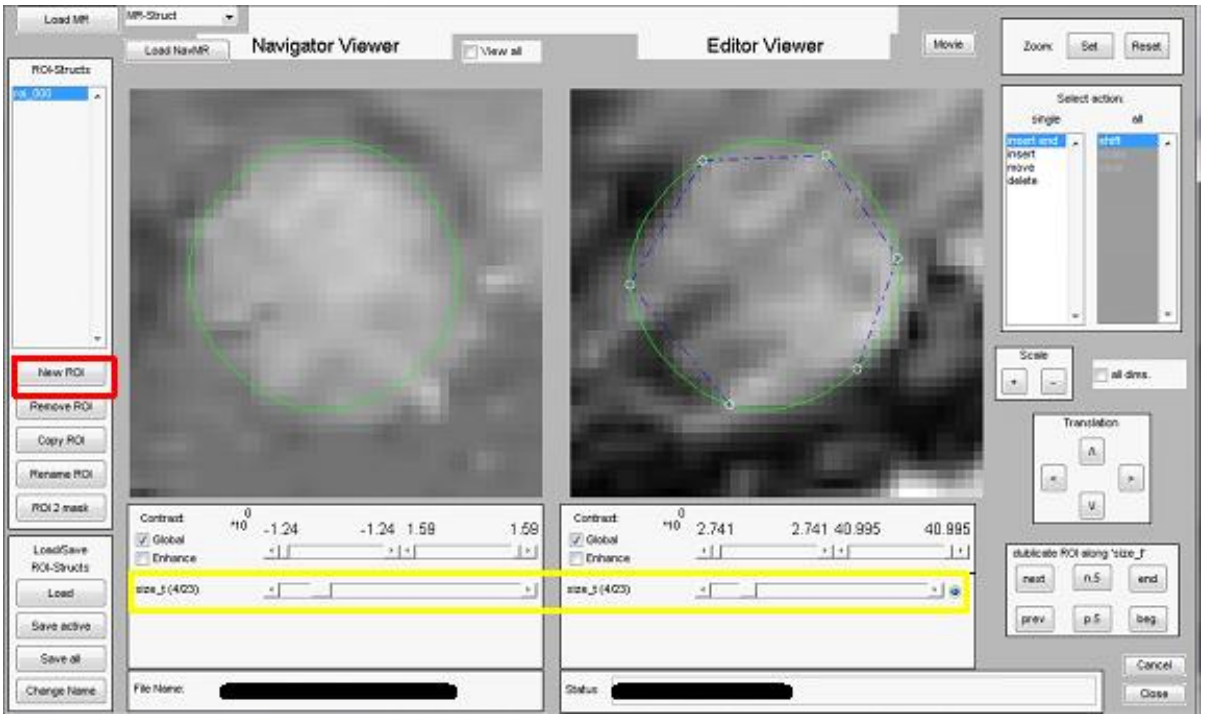

Figure 14: "ROI-tool" user surface: with navigator and editor view; vessel area (green circle) could be cropped individually at each time frame of the cardiac cycle; here, peak systole was chosen, phase 4 (yellow box). Data from a 40-year old healthy male volunteer at middle AAo. "Roi-tool" screenshots.

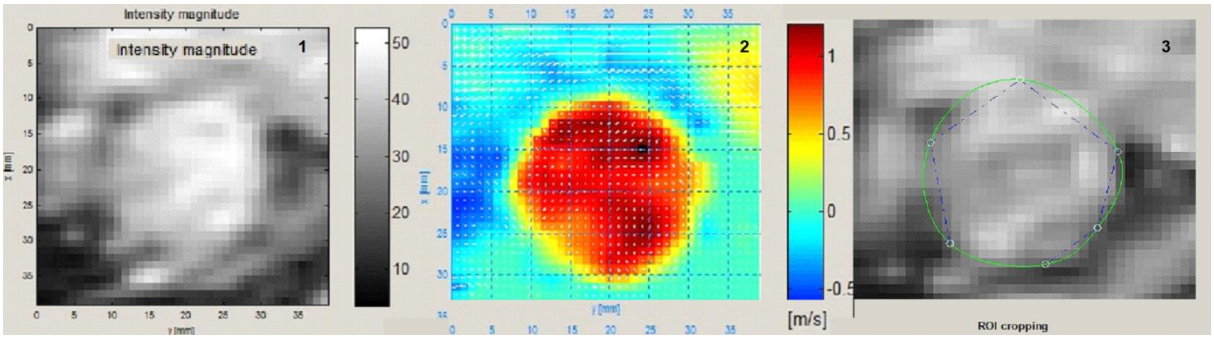

Figure 15: Workflow of vessel wall definition: *panel 1*) magnitude image; *panel 2*) 2D velocity profile; *panel 3*) Definition of region of interest (ROI). Data derived from a 25-year old female volunteer during peak-systole in the middle AAo. "Flow_tool" screenshots.

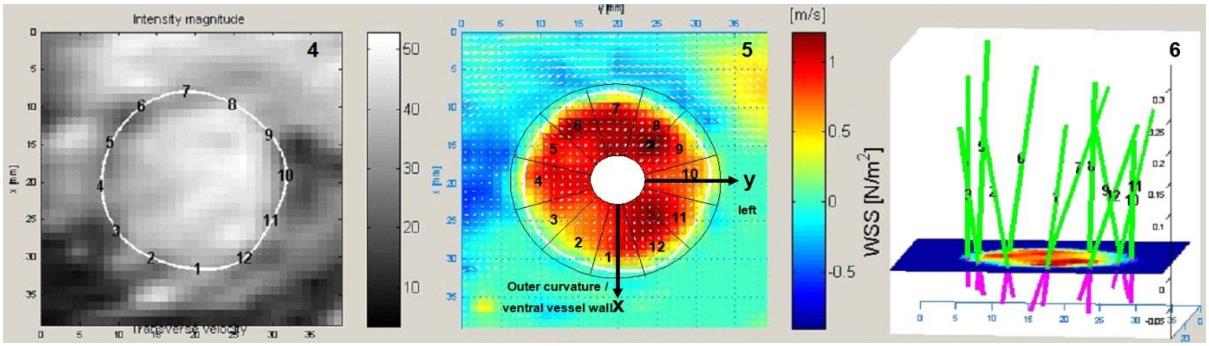

Figure 16: Workflow WSS quantification: *panel 4*) defined aortic area with vessel wall segmentation; *panel 5*) 2D velocity profile with supporting coordinate system for orientation; *panel 6*) WSS at vessel wall given as mean over one cardiac cycle (green baulks), one for each vessel wall segment; pink baulks represent OSI (Oscillatory shear index). Data derived from a 25-year old female volunteer at peak systole in the middle AAo. "Flow_tool" screenshots.

Given that, "Flow_tool" automatically computed flow and wall shear stress metrics in a standardized manner (Stalder 2009, pages: 78-80), *figure 17 and 18.*

Derived data were given as mean and as spatial-temporally resolved values, *figure 17 and 18.* That means that results were calculated as mean for the entire cardiac cycle but also temporally resolved at each single time step, e.g. during peak systole or end diastole. Any desired time frame could individually be selected on the interactive user surface, *figure 13 and figure 17.*

This further means, that also spatially-resolved information could be computed as mean value of the entire vessel circumference (*figure 18*) or particularly in one of 12 sub-segments (*figure 16*). Segments were numerated from 1 to 12, where 1 was by definition the direction of the X axis, the ventral aortic wall, *figure 16 and 19*.

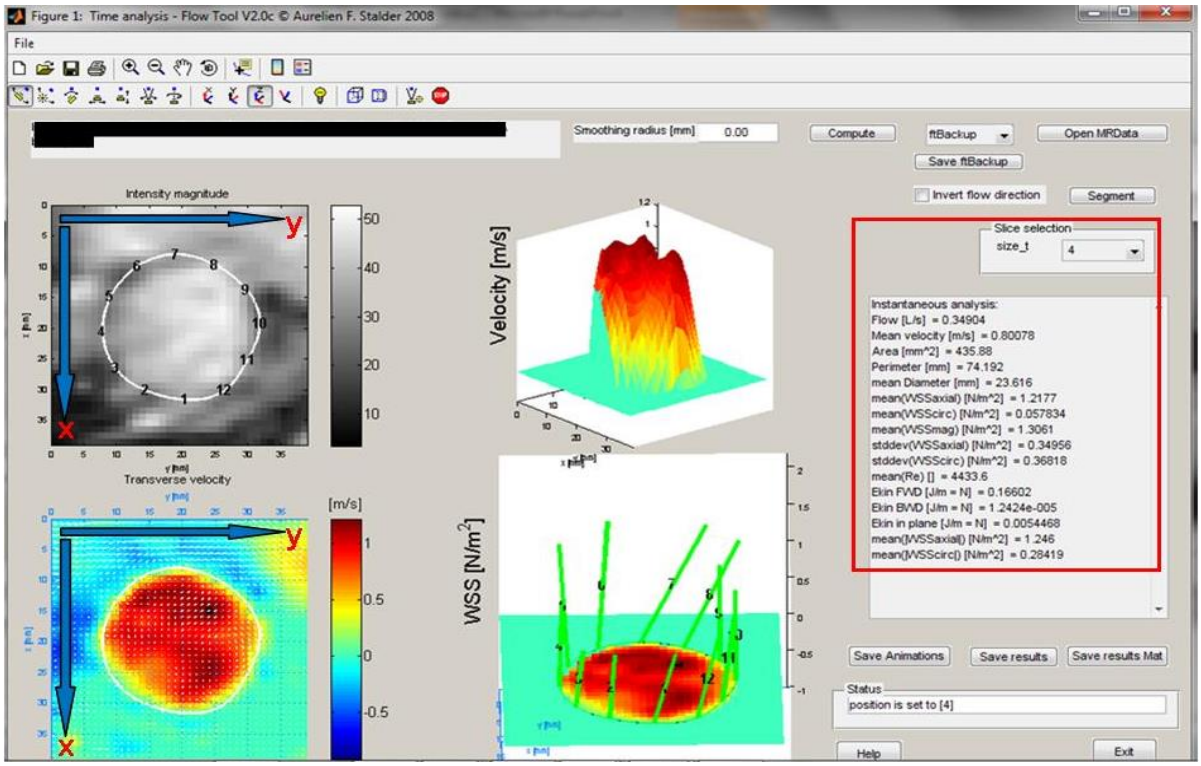

Figure 17: "Flow_tool" instantaneous analysis. Peak systole (here phase 4, red box); the inter-active window enabled selecting of an arbitrary time-frame of the cardiac cycle, from systole to diastole. Red box: calculated values of velocity and wall shear at peak systole. 2D (down left) and additional 3D velocity profile (centre top) at peak systole; centre bottom shows wall shear stress vector profile (green bars) in each of the 12 segments (numeration as given in *figure 16*). Saving options down right (backup, animation, results). "flow_tool" screenshot.

Wall shear stress data were calculated for WSS_{axial}, WSS_{circ} , and $WSS_{magnitude}$. Values were acquired from each subject of both study and control group at middle and distal AAo. Results were saved as

"backup files" in MATLAB format. Graphical results were saved as animations. Numerical data were stored as "Excel" files (Microsoft Excel ™), *figure 17*.

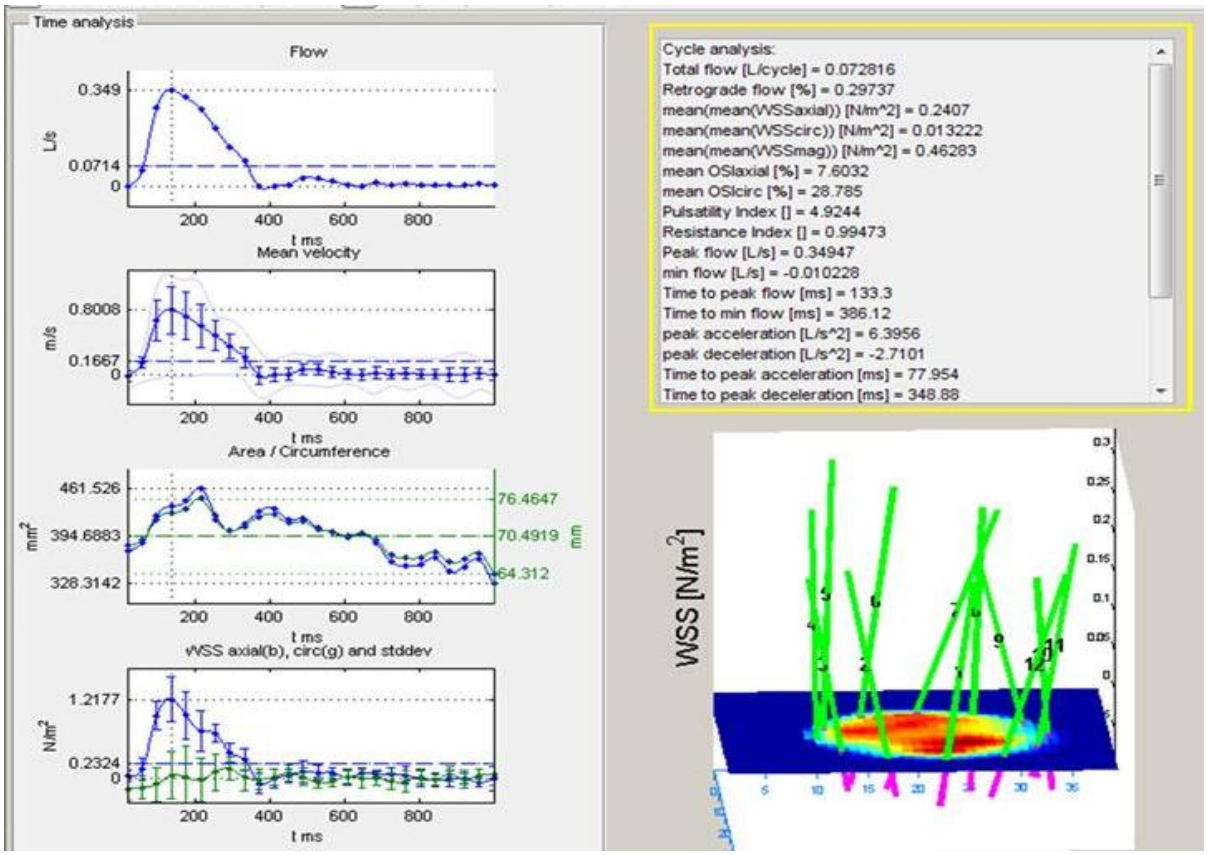

Figure 18: "Flow_tool" cardiac cycle analysis: the window provides global parameters and time curves over one cardiac cycle. Left panel presents time resolved results of flow, mean velocity, vessel area, WSS axial and WSS circ. The box on the right depicts flow and wall parameters. Average WSS vectors (green bars) and OSI (pink bars) are illustrated downright. For matters of graphical representation OSI of each of the 12 segments is opposed to WSS.

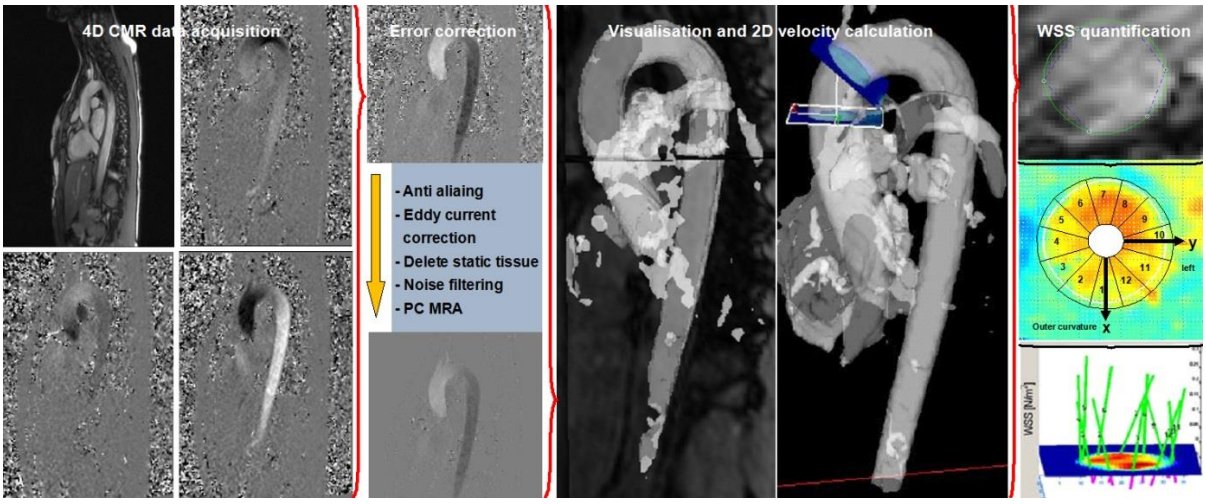

Figure 19: Work flow of 4D CMR data acquisition, pre-processing and WSS quantification

2. 2. 5 Statistical Methods

For statistical matters different tests were applied to analyse results for significance or non-significant differences. Thus, this section is subdivided into basic population data statistic and statistical calculation of WSS parameters.

A p-value of $p \leq 0.05$ was considered to be significant. “Statview” (Statview 5, Abacus Cooperation, USA) was chosen for computational analysis.

2. 2. 5. 1 Basic Data of the Study Populations

Statistical analysis of age, height and weight between BAV and TAV population (*table 4*) was done with paired t-test. These values were normally distributed.

Body surface area (BSA), blood pressure and aortic diameter between each sex and age matched pair were analysed applying Wilcoxon signed-rank test. A non-normal distribution of values made this non-parametric testing necessary. Among non-parametric tests Wilcoxon signed-rank test was chosen as it not requires assumptions about the distribution and allows analysis of paired values.

2. 2. 5. 2 Wall Shear Stress Parameters

Numerical values of WSS_{axial}, WSS_{circ}, and $WSS_{magnitude}$ were statistically analysed applying Wilcoxon signed-rank test. Data were analysed between all 18 age and sex matched couples.

3 Results

3. 1 Basic Data of Study and Control Group

Twenty-two of 26 4D CMR examinations amongst invited study subjects derived usable data. Measurement error occurred in four cases for unknown reasons and did provide insufficient 4D CMR data. Under volunteers, three examinations failed. Causes for that were ascribed to hardware failure of the computer interface. For logistical reasons examination could not be repeated in these four cases. Therefore patient and control group were together amounted to 36 participants.

Eighteen patients with BAV but none concomitant vessel disease were compared with a group of 18 sex and age matched volunteers with TAV (*table 4*).

Statistical analysis of demographical data in control and patient population										
Criteria		Controls with TAV		Patients with BAV			Controls with TAV		Patients with BAV	
		n = 18		n = 18			n = 18		n = 18	
		mean	SD	mean	SD	p	median	range	median	range
Age	yrs	26.1	± 8.0	26.20	± 8.4	0.8781	25.0	8 - 42	25.0	10 - 44
Height	cm	174	± 13.8	175	± 12.1	0.5904	174.0	130 - 188	176.5	138 - 192
Weight	kg	68.1	± 16.4	68.9	± 14.9	0.6888	67.5	29 - 95	67.5	30 - 94
BSA	[m²]	1.8	± 0.3	1.80	± 0.2	0.5294	1.8	1.0 - 2.2	1.8	1.1 - 2.2
P_{sys}	[mmHg]	107.1	± 7.7	110.9	± 9.6	0.2209	107.0	94 - 122	109.0	98 - 128
P_{dia}	[mmHg]	59.7	± 11.2	65.7	± 11.6	0.5321	58.0	47 - 82	65.0	46 - 83
Dmax corrected	[cm/m²]									
Bulbus aortae		1.62	± 0.23	1.76	± 0.24	0.1771	2.10	1.6 - 2.9	2.3	1.9 - 3
Ascending aorta		1.57	± 0.2	1.89	± 0.26	**0.0033**	2.1	1.6 - 2.4	2.6	1.7 - 3.2
Descending aorta		1.08	± 0.11	1.05	± 0.17	0.4851	1.4	1.1 - 1.7	1.4	1.1 - 1.6

Table 4: Demographical data of study and control group: absolute results are displayed as mean values plus/minus standard deviation (SD) and p-value (p); median and range of values are depicted right-hand; TAV = tricuspid aortic valve; BAV = bicuspid aortic valve; BSA = body surface area; P_{sys} = systolic blood pressure; P_{dias} = diastolic blood pressure; Dmax corrected = maximum diameter normalized to BSA (Roman et al. 1989, page: 510). Statistical analysis: paired t-test for age, height and weight; Wilcoxon signed-rank test for BSA, blood pressure and aortic diameter.

There was no significant difference in age, sex, height, weight, BSA, systolic or diastolic blood pressure (P_{sys}, P_{dias}). The mean values (mean), standard deviation (SD), median, range and p - values are listed in *table 4*.

Despite careful patient group acquisition and strict exclusion criteria, however, significant difference of mean ascending aortic diameter (corrected for BSA) was found between BAV (1.89 cm/m² ± 0.26) and TAV group (1.57 cm/m² ± 0.2) (p = 0.0033). Diameter of the aortic bulb (p = 0.1771) and DAo were not significantly different (p = 0.4851).

3. 2 Wall Shear Stress (WSS)

As explained before WSS can be separated into its axial and circumferential component (*figure 2 and 3*). For that reason, the results of WSS $_{axial,}$ WSS $_{circ,}$ and WSS $_{magnitude}$ are described in sub-sections. Wall shear stress at the vessel wall of the AAo was quantified using "flow_tool" (section 2.2.5.2).

3. 2. 1 Axial Wall Shear Stress (WSS $_{axial}$)

Mean WSS $_{axial}$ along the middle AAo was significantly lower in the BAV group (0.187 N/m² ± 0.062) than in the control group (0.230 N/m² ± 0.06) (p = 0.0074). Measurement of WSS $_{axial}$ in the distal AAo before the brachiocephalic trunk (BCT level) yielded no significant differences between BAV group (0.268 N/m² ± 0.081) and TAV group (0.28 N/m² ± 0.056) (p = 0.3958), *figure 20.*

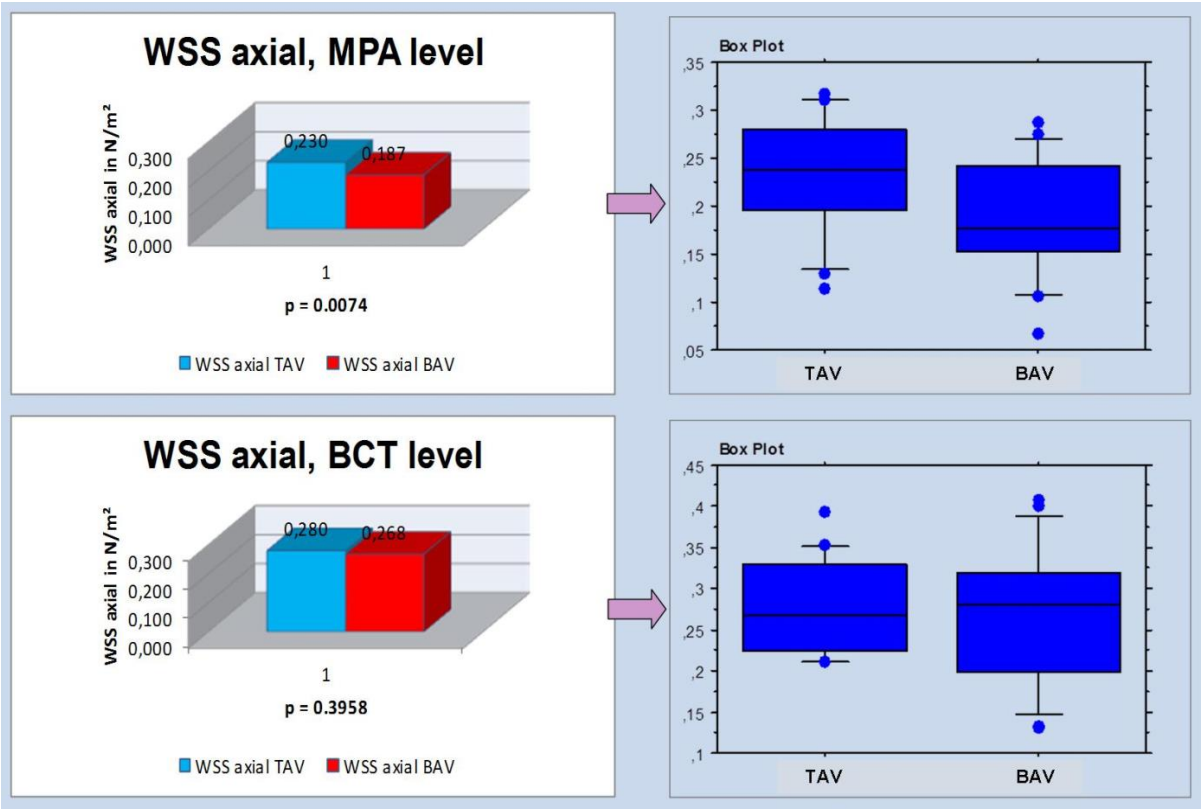

Figure 20: WSS $_{axial}$, mean values, measured in the ascending aorta at MPA level, middle AAo (upper panels) and BCT level, distal AAo (lower panels); left side: diagrams with average values of WSS $_{axial}$ in TAV (blue columns) and BAV (red columns), statistical difference given with 'p'; p - values were derived using Paired Wilcoxon-White-test. Right side: box plots of all values; MPA - main pulmonary artery; BCT - brachiocephalic trunk; Box plots and p – values were calculated with Statview (Statview 5, Abacus Cooperation, USA).

3. 3. 2 Circumferential Wall Shear Stress (WSS $_{circ}$)

Mean WSS $_{circ}$ of the total vessel circumference in the middle AAo was found to be significantly higher in the BAV group (0.229 N/m² ± 0.153) compared to TAV group (0.038 N/m² ± 0.075) (p = 0.014).

Quantification of mean WSS $_{circ}$ at the distal AAo wall also showed higher outcomes in the BAV group (0.183 N/m² ± 0.137) compared to TAV group (0.066 N/m² ± 0.067), and this diversity also was significant (p = 0.0084), *figure 21*.

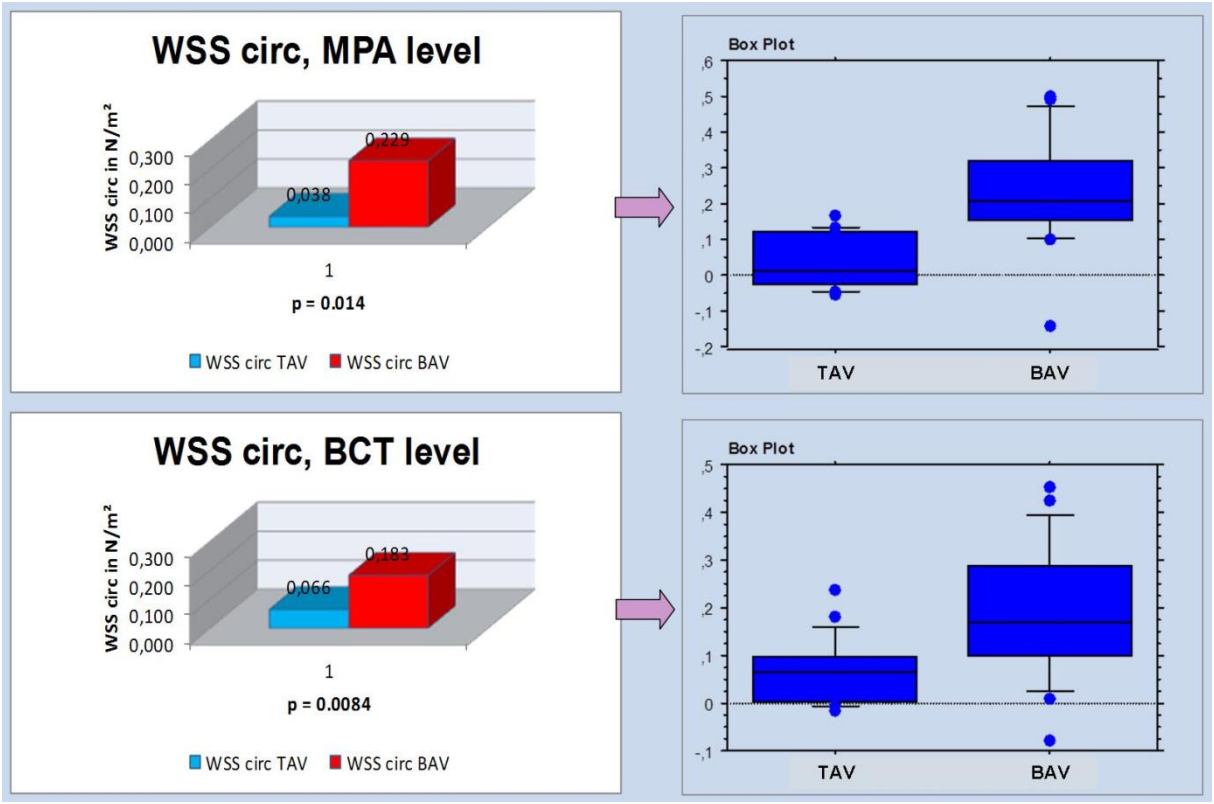

Figure 21: WSS $_{circ}$, mean values, measured in the ascending aorta at MPA level, middle AAo (upper panels) and BCT level, distal AAo (lower panels); left side: diagrams with average values of WSS $_{circ}$ in TAV (blue columns) and BAV (red columns), statistical difference given with 'p'; p - values were derived using Paired Wilcoxon-White-test. Right side: box plots of all values; Box plots and p - values were calculated with Statview (Statview 5, Abacus Cooperation, USA).

3. 3. 3 Magnitude of Wall Shear Stress (WSS $_{magnitude}$)

WSS $_{magnitude}$ measured in the middle AAo at MPA level was significantly lower in the TAV group (0.49 N/m² ± 0.08) in comparison to the BAV group (0.588 N/m² ± 0.165) (p = 0.0279).

In the distal AAo, difference was not significant though (p = 0.145). Anyway, values appeared to be slightly lower in the TAV group (0.523 N/m² ± 0.106) than in the BAV group (0.589 N/m² ± 0.134), *figure 22.*

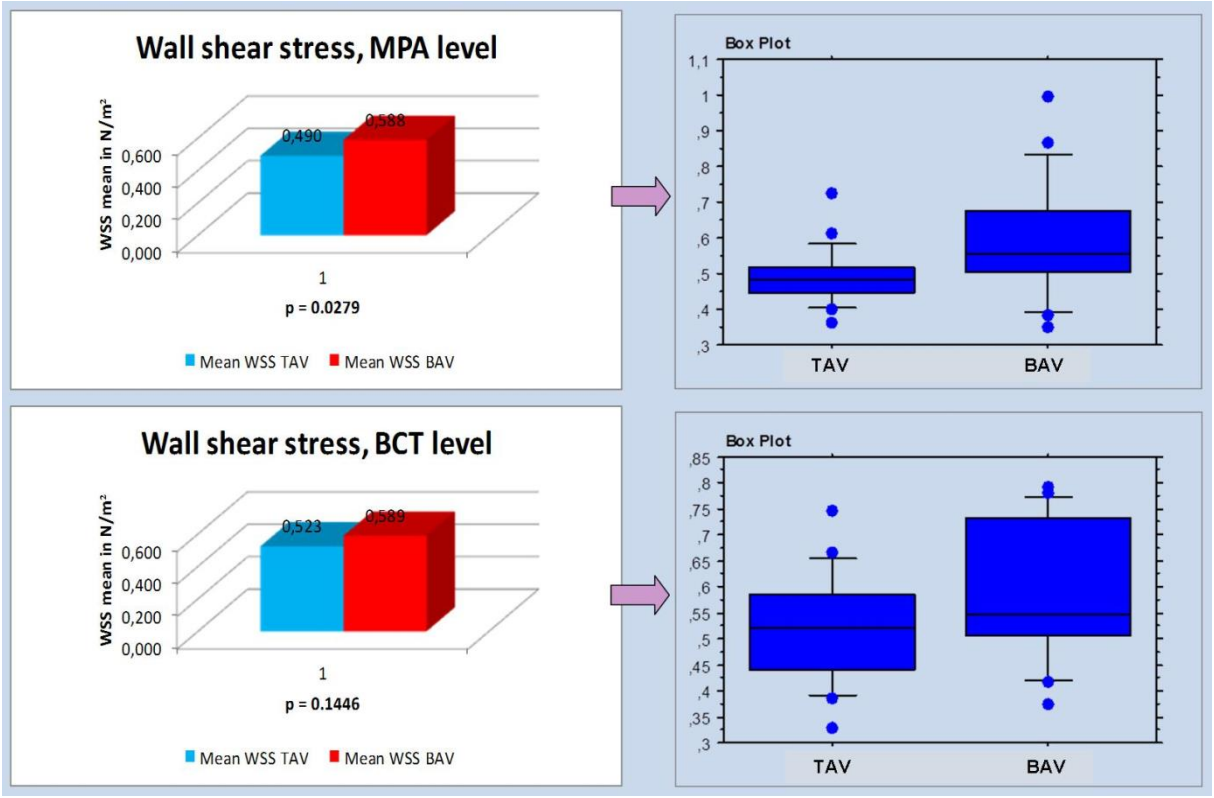

Figure 22: Numerical results of wall shear stress quantification in the middle (top) and distal ascending aorta (below). Left side: diagrams with average values of WSS $_{magnitude}$ in TAV (blue columns) and BAV (red columns), statistical difference given with 'p'; p - values were derived using Paired Wilcoxon-White-test. Right side: box plots of all values; Box plots and p - values were calculated with Statview (Statview 5, Abacus Cooperation, USA).

Hence, wall shear stress (WSS $_{magnitude}$) acting on the aortic vessel wall of the middle AAo was crucially higher among subjects with BAV than those with TAV. However, this difference was limited to the middle ascending aorta and was not found more distally, *table 5.*

Wall shear stress values, measured in the ascending aorta							
Parameter	Unit	mid AAo	mid AAo		distal AAo	distal AAo	
		TAV	BAV	p	TAV	BAV	p
WSS axial	N/m²	0.23 (0.0601)	0.187 (0.0618)	0.0074	0.28 (0.0562)	0.268 (0.0813)	0.3958
WSS circ	N/m²	0.038 (0.0749)	0.229 (0.1533)	0.014	0.066 (0.0669)	0.183 (0.1375)	0.0084
WSS mag	N/m²	**0.49 (0.0802)**	**0.588 (0.1652)**	**0.0279**	0.523 (0.1062)	0.589 (0.1342)	0.1446

Table 5: Results of wall shear stress (WSS) measurement, summarized; standard deviation in brackets. p = p-value, calculated with Wilcoxon signed-rank test, TAV = tricuspid aortic valve, BAV = bicuspid aortic valve, mid/distal AAo = mid/distal ascending aorta, circ = circumferential, mag = magnitude.

Figure 23 shows graphical results of flow and WSS $_{magnitude}$ quantification as mean value over the entire cardiac cycle in two eight and ten year old females. Even though aortic diameter in the TAV subject were wider than in the matched BAV individual, still flow and WSS are markedly altered in

the BAV subject. *Figure 24* depicts opposed WSS vectors of three more sex and age matched pairs the in middle ascending aorta.

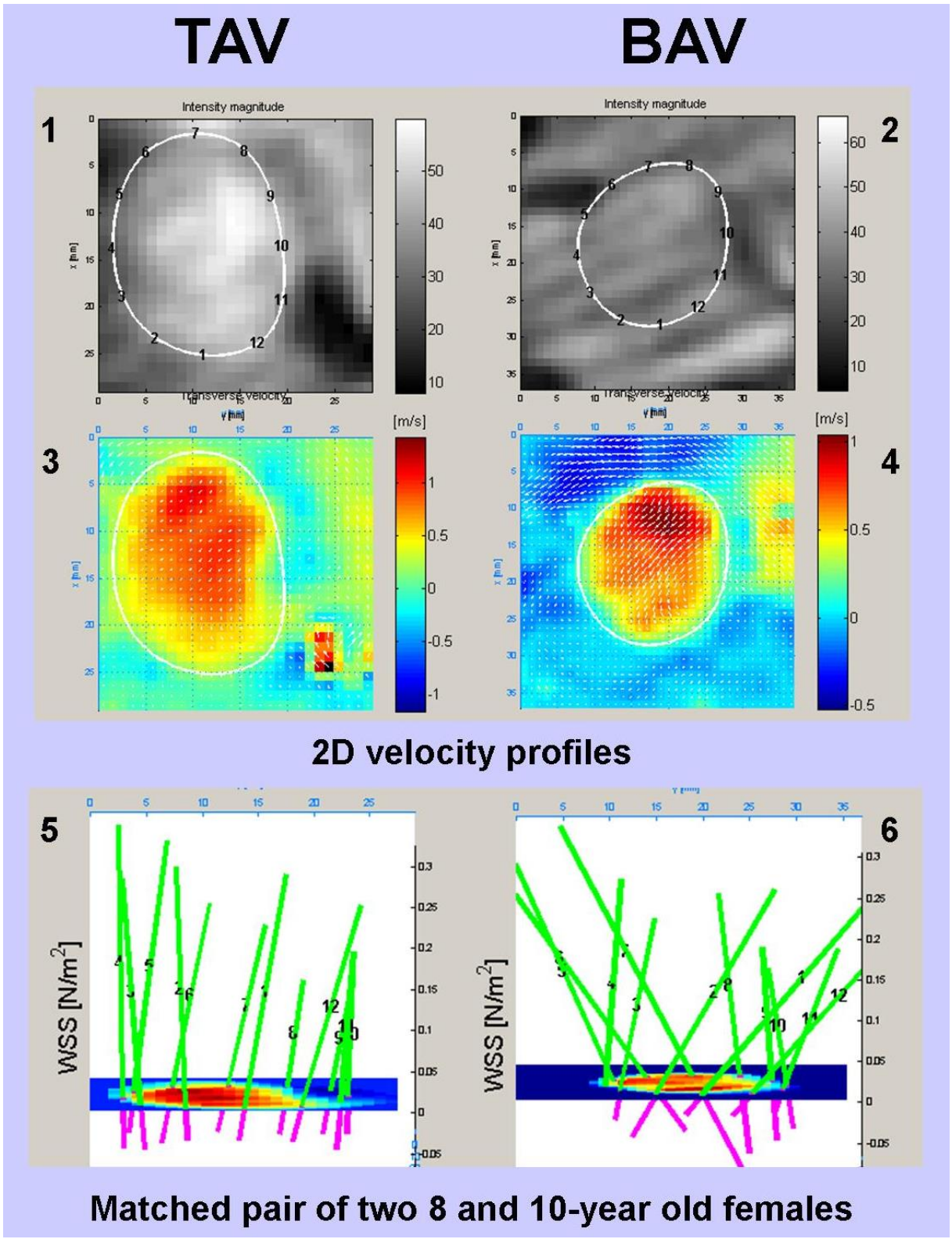

Figure 23: Graphical results of flow and WSS quantification in the middle AAo in two eight (TAV) and ten year old (BAV) females. 2D velocity profiles (panels 3 and 4) show unequally distributed flow fields. Panels 5 and 6 depict WSS profiles. Green bars present WSS $_{magnitude}$ over cardiac cycle, numeration as in figures before. Pink bars = OSI. "Flow_tool", screenshots.

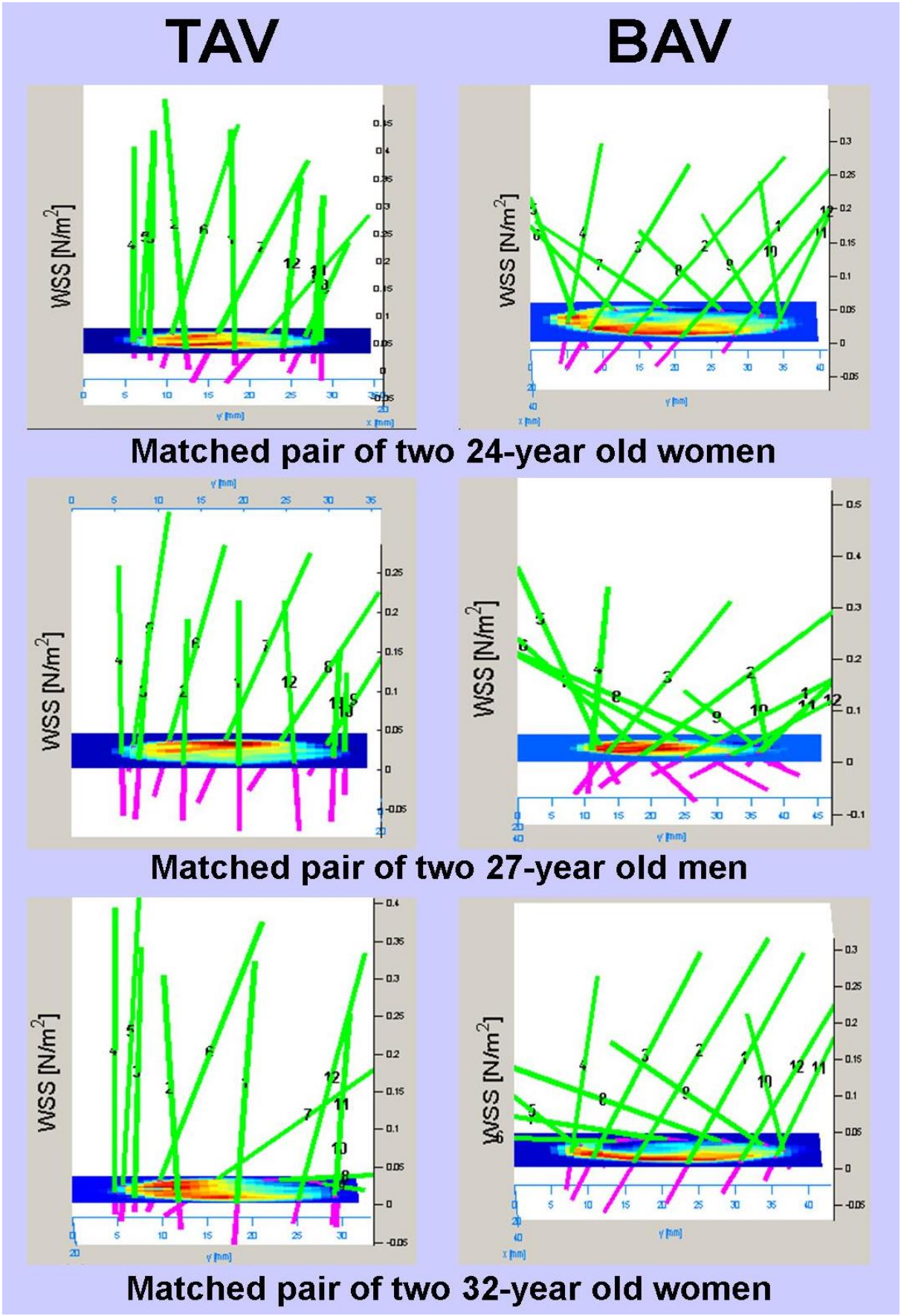

Figure 24: WSS $_{magnitude}$ vector profiles; middle AAo. Three sex and age matched pairs of BAV and TAV. WSS in the BAV group is evidently less axial and more directed onto the aortic wall. Green bars present magnitude of WSS during one cardiac cycle; numeration of bars as in figures before. Pink bars represent OSI over time. "Flow_tool", screenshots.

4 Discussion

4. 1 Patient Group Design

4. 1. 1 Criteria of Inclusion and Exclusion

The purpose of this study was to compare shear stress at the ascending aortic wall of BAV patients to control subjects with TAV. As flow forces like shear stress are dependent on haemodynamic conditions, criteria for inclusion or exclusion were chosen to be particularly strict as to guarantee equal and undisturbed flow circumstances in all participants. Therefore, previous cardiovascular surgery as well as congenital malformations of the heart, the pulmonary artery or the aorta led to exclusion. The same counted for diagnosis of arterial or pulmonary HTN as well as antihypertensive medication. And, most importantly, aortic regurgitation or/and aortic stenosis were criteria leading to exclusion.

This was performed to ensure the often cited conditions “independent of any hemodynamically significant valvular disease” in the AAo in both patients and controls (Braverman et al. 2005, page: 498; Bonow et al. 2008, page: e 559). In addition to the strict criteria patients were sex and age matched to avoid confounders of aging or gender.

Barker et al published very interesting results regarding the same topic in 2010. However, their study and control groups were not age matched. Thus, to the author’s knowledge this study was the first investigating in vivo WSS values in the AAo of an age and sex matched population of people with BAV and TAV.

Note that subtypes of BAV (type 1, 2 and 3) were not sub-classified particularly although valve opening shape is considered to be different. This may be seen as a limiting factor.

4. 1. 2 Number of Patients

The number of 18 patients may sound very little as approximately 0.5-2 % of the human population does present with BAV (Roberts 1970, page: 78; Basso et al. 2004, page: 663; Fedak et al. 2003, page: 900). This is possible to explain with two main facts.

First, many patients with normally functioning BAV, as for the study required, do not show any clinical presentations and are only diagnosed by chance during routine physical exam (Braverman et al. 2005, page: 483). Thus, these patients are typically neither under medical treatment nor listed in any medical database for the reason of BAV. Furthermore, the inclusion criteria of the presented study were relatively strict. Most of the patients with BAV found in our database did have other pathologies of the heart, such as ventricular septum defect (VSD), aortic stenosis (AS > grade I), aortic insufficiency (AI > grade I), Coarctation of the aorta (CoA) or prior undergone heart surgery.

Facing the first fact and that “20% and possibly up to 50% of subjects with BAV have additional congenital cardiovascular malformations” (Braverman et al. 2005, page: 479) it is comprehensible that finding study subjects who meet the inclusion criteria was challenging.

Secondly, getting in touch with potential candidates for the study was hampered by false or missing contact data. Reasons for this may be the registration date, which was more than 20 years ago in some cases. On the other hand, the changeover from non-digital to digital administration and data management in this period plays an important role as well.

Taking the latter two sections in account, the low number of patients may become rather understandable. Nevertheless, this may be seen as a limitation and studies with higher numbers of participants are needed.

4. 2 Methods

CMR is an officially accepted method in cardiac diagnosis in patients with thoracic aortic disease (ACCF/AHA/AATS/ACR/ASA/SCA/SCAI/SIR/STS/SVM 2010, page e43). However, wall shear stress quantification from CMR velocity data is a new approach still at an early stage.

The derived WSS data must be seen as estimated values which are correlated to actual WSS. (Stalder et al. 2008, page: 1228). However, the high consistency in healthy subjects or compared to computational fluid dynamic (CFD) studies points out the potential to compare WSS estimations from volunteers to those of BAV subjects (Bieging et al. 2011, page: 596).

It should also be noticed that pre-processing strategies of WSS quantification were not completely performed in a standardized manner. Some error correction was undertaken individually and observer-based and might have led to minor errors in data calculation. However, pre-processing was performed blinded and by only one person.

The 4D CMR scan time of approximately 20-40 minutes did not allow for repeated measurement, thus inter-scan reproducibility was not possible to assess. Anyway, the method was used by others and is widely accepted (Stalder et alt. 2008, page: 1219; Barker et alt. 2010, page: 789).

Both facts may be seen as a limitation of the methodical procedure. However, pre-processing and WSS quantification were performed after instructions by Markl and associates.

4. 3 Basic Results in the Study Population

4. 3. 1 Aortic Diameter

Significant difference in diameter of the middle AAo was found between patients and control group despite careful study group design. On the other hand, there was no statistically significant difference at the level of the aortic bulb or the DAo, *table 4*.

Even though, these findings were not optimal as study and control group design had the goal to compare almost equal individuals, they principally confirm earlier publications arguing that dilation of the AAo occurs not age related and more often in patients with BAV than in healthy subjects (Hahn et al. 1992, page: 236). So, finding enlarged diameters in the study group was not totally unexpected and underlined the theory that even asymptomatic patients do already show widened aortic diameters. Since demonstrably no “hemodynamically significant aortic stenosis or aortic regurgitation” (Bonow et al. 2008, page: e559) were present among the individuals they were, nevertheless, assessed to be appropriate for further examinations.

4. 4 Results of WSS Quantification in the Middle of the AAo

The axially directed wall shear stress was found to be significantly lower in BAV patients compared to TAV subjects in the middle AAo ($p = 0.0074$), whereas circumferentially aligned wall shear stresses were significantly higher in BAV than in TAV in the same area ($p = 0.014$).

Interestingly, these results correlate with previously acquired data at our department (Meierhofer et al. 2010, poster presentation). Meierhofer could show that right helically, strongly twisted flow in the AAo was significantly more often seen in BAV than TAV.

Remembering *illustrations 2 and 3,* the obtained numerical and graphical results of measured WSS reflect these findings. While helical flow was related with high circumferential and low axial WSS, straight flow patterns correlated with very low circumferential but higher axial WSS. These findings seem to validate Stalder's method to quantify WSS (Stalder et al. 2008, pages: 1218-1231) applied in this study.

Thus, one can say that circumferential wall shear stress values may be seen as a numerical quantity for helical flow.

As explained in the introduction magnitudinal WSS ($WSS_{magnitude}$) is the vector sum of axial and circumferential shear. $WSS_{magnitude}$ was found to be significantly higher in the middle AAo in BAV population ($p = 0.0279$). The graphical outcomes of wall shear quantification in *figure 23 and 24* are explicitly mirroring the numerical results and show obvious differences in both groups. The instantaneous vector profile of WSS at peak systole only showed slightly distracted shear vectors in TAV subjects, whereas vector direction of the matched middle AAo in BAV were obviously counter-clockwise twisted (*figure 23, 24*). Also, mean $WSS_{magnitude}$ (averaged over the cardiac cycle) gave a clear impression of how shear forces differed between both groups.

Despite the given results of WSS_{axial} and WSS_{circ} their vector sum ($WSS_{magnitude}$) was not automatically expected to be different. Low circumferential and high axial shear in healthy people opposed to high circumferential and low axial shear stress in BAV patients could have revealed equal vector sums in both groups.

But they did differ. When looking at the values of axial and circumferential WSS in both groups and especially at their relation to each other (*figure 25*) one may better understand these results. While axial WSS in the TAV group appeared to play the major role within the relation of shear components (0.23 versus 0.038 N/m^2, WSS axial vs. WSS circ), in BAV this relation was almost balanced (0.178 versus 0.229 N/m^2, WSS axial vs. WSS circ), *figure 25*.

Although axial shear stress in BAV was lower than in TAV the immense higher circumferential stress found in BAV patients resulted in significantly higher vector sums of $WSS_{magnitude}$ at the middle ascending aortic wall. This is exactly the anatomical region where the aorta in BAV dilate most often (Bauer et al. 2006, pages: 594-600).

Note that $WSS_{magnitude}$ was not significantly different in the distal AAo.

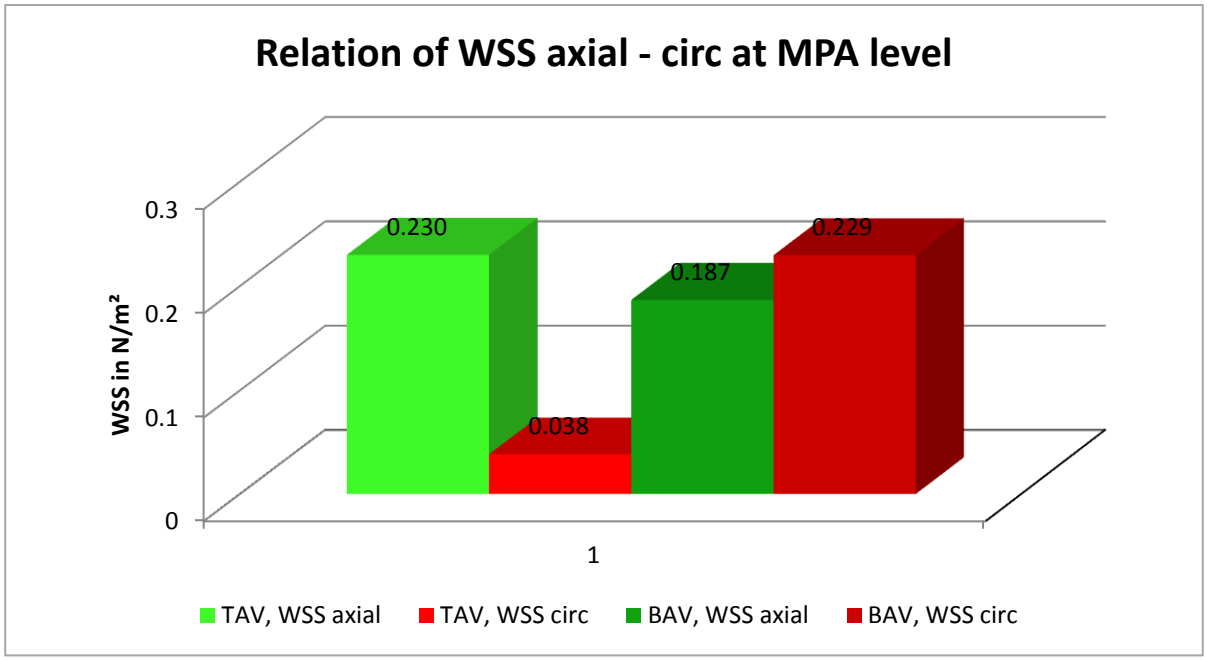

Figure 25: Relation of WSS $_{axial}$ (light green column) to WSS $_{circ}$ (red column) in the TAV group confronted with WSS $_{axial}$ and WSS $_{circ}$ (dark green and dark red columns) in the BAV group.

One might argue that altered flow and increased wall shear stress values might be determined by larger aortic diameters found in the BAV group. But this suspicion can specifically ruled out on the example of one matched pair (*figure 23*) where the aorta of an healthy eight-year-old female with TAV was larger than the aorta of its opposed ten-year-old female with BAV. Even though aortic dimensions were bigger in the TAV subject, still flow and WSS was strongly altered in the BAV subject.

This supports the idea that flow and WSS is alterd by the valve and not by vessel layer or vessel size.

4. 5 Dilation of the Ascending Aorta in Subjects with BAV

BAV patients suffer more often from ascending aortic dilation, aneurysm, dissection or rupture than healthy subjects (Nistri et al. 1999, page: 19). In fact, the BAV population of this study showed enlarged middle ascending aortic diameter (section 3.1), underlining this theory. Commonly known reasons for the development of dilation and aneurysm in the ascending aorta are atherosclerosis, connective tissue disorders like Marfan (MS), Ehlers-Danlos syndrome or Loeys-Dietz syndrome, inflammatory diseases like Takayasu arteritis or simply aging (Herold 2007, pages: 724-726). Another main factor proven to be very important is arterial hypertension (HTN) (Renz-Polster et al. 2008, pages: 236 ff.). But also “mechanical effects of the high velocity systolic jet on the aortic wall” (Bauer

et al. 2006, page: 600) are considered to be responsible, especially in patients with aortic stenosis. The latter two may primarily be described as haemodynamic factors. Principally, haemodynamic as a cause for ascending aortic dilation and aneurysm are widely accepted and listed in medical literature (Wiener et al. 2004, page: 1483).

Anyway, pathological haemodynamic in patients with bicuspid aortic valve is still matter of intensive debates. Dilation of the aorta with its consequences occurs earlier and more often in life of BAV patients than in people with TAV (Braverman et al. 2005, page: 500; Roberts, Roberts 1991, page: 716). As this happens despite the absence of arterial HTN, AS, MS, inflammatory diseases, step by the step, a theory stating an eventually existing inborn connective tissue defect in BAV was raised.

In 1957 McKusick wrote about the correlation of BAV and "Erdheim's cystic media necrosis" suggesting this aortic wall abnormality was "result of hemodynamic stress" (McKusick et al. 1957, page: 1957). Fourteen years later he challenged his own theory after having found changes in the media of vessels "where hemodynamic stress should be less of a factor" and uttered a "developmental defect" (McKusick 1972, page: 1026). While Lindsay substantiated this theory in his summary in 1988 he also said, on the other hand, that wall abnormalities alone "cannot be taken as conclusive evidence of intrinsic weakness" (Lindsay 1988, page: 182). However, a genetic defect of the aortic wall appeared for many to be the most likely explanation and a lot of investigations should follow.

Neural crest cell defects in the aortic wall were suggested to be associated with or even causative for aortic dilation in BAV (Schievink, Mokri 1995, pages: 1935-1940). Evidence of similarity in tissue abnormalities in the media of patients with MS and those with BAV could be provided by Niwa et associates in 2001; in BAV even "irrespective from the functional state of the valve" (Niwa et al. 2001, pages: 394, 396). Fedak argued in 2002 that "matrix disruption and smooth muscle cell loss" may result in structurally weakened aortic wall (Fedak et al. 2002, page: 902) while also linking these findings with those in Marfan patients.

Boyum et al faced the issue from another point of view (Boyum et al. 2004, pages: 686-691). They highlighted aortic aneurysms in subjects with TAV compared to those with BAV and found that MMP activity seems to be higher in BAV aortic aneurysms compared to TAV aortic aneurysms concluding a "genetic alteration in MMP metabolism" could lead the aortic disease in BAV patients (Boyum et al. 2004, page: 691).

Even though, none of these studies could finally prove a genetic tissue abnormality being responsible for the frequently occurring aortic pathology in BAV patients a hemodynamic explanation was ruled out little by little. And the believing in a genetic defect was carried further even more ever since

Pachulski and Hahn had shown in 1991 that ascending aortic root dilation after BAV appeared to occur despite normally functioning valves, in absence of AS or AI (Pachulski et al. 1991, page: 782; Hahn et al. 1992, page: 286). Keane et al underlined that in 2000 with their publication demonstrating that dilation in the AAo is associated with BAV "out of proportion" to valvular lesions (Keane et al. 2000, page: 38).

However, a heart valve does not necessarily have to be stenotic or insufficient to be abnormal. A congenitally different valve formation must also be seen as an abnormal haemodynamic circumstance. And two cusps instead of normally three should also be considered as a valvular lesion.

Anyway, investigators like Aboulhosn and Child favoured more and more the theory of a genetic disorder (Aboulhosn, Child 2006, page: 2415). Braverman and colleagues mentioned in their large review "The Bicuspid Aortic Valve" the haemodynamic theory, but did principally emphasize an underlying developmental tissue defect (Braverman et al. 2005, pages: 470-522). Basing on that and Nataatmadja's findings of increased smooth muscle cell apoptosis in the AAo behind BAV, also the "2008 Focused Update Incorporated into the ACC/AHA 2006 Guidelines for the Management of Patients with Valvular Heart Disease" do only speak of "disorders of vascular connective tissue (…) in absence of hemodynamically significant aortic stenosis or aortic regurgitation" (Bonow et al. 2008, page: e559; Nataatmadja et al. 2003, page: 329-334).

As already mentioned, given all the named findings for many investigators a definite correlation of genetic tissue defect and aortic dilation in BAV seems to be evidenced.

But not all do think so. Gunteroth critically reviewed the 2008 updated guidelines suggesting that the kind of turbulence caused by a normally functioning BAV might have effects as well despite the absence of stenosis or regurgitation (Guntheroth 2008, page: 109). Thereby he is one of the few still arguing with a haemodynamic explanation for dilation in BAV. Thus, his principal opinion is that a heart valve does not necessarily have to be diseased to cause altered flow and changed haemodynamic in the ascending aorta. And there are many reasons to believe that.

In general we do know for a long time that aortic valves may cause turbulent flow, never mind if normal or diseased (Stein, Sabbah 1976, page: 65). In 2004, Robicsek at al showed experimentally that the opening shape of BAV was different to TAV. In addition, they demonstrated abnormal vortices and currents in blood flow after normally functioning bicuspid valves. They furthermore stated that the degree of turbulence was not necessarily relative to the degree of stenosis (Robicsek et al. 2004, page: 184). In 2006, when echocardiographically comparing stenotic bicuspid and tricuspid aortic valves Bauer et associates found despite equally widened ascending aortas and no

age differences among the patients significantly higher peak velocities at the anterior-lateral aortic wall of BAV patients (Bauer et al., pages: 219-220).

This introduces again the question whether stenosis or/and regurgitation in aortic valves are the only relevant conditions for blood flow haemodynamic or if the style of leaflet opening and closure may significantly contribute as well. Facing this, one may better understand Gunteroth's thoughts. But how may one find more evidence for this theory?

Improvements in cardiac imaging might bring insightful inputs into this discussion of blood flow and haemodynamic influenced by the aortic valve. In the nineties Kilner and Bogren described slightly right handed helical flow patterns in the AAo of healthy individuals seen in three dimensional visualisations of aortic blood flow using CMR (Kilner et al. 1993, pages: 2235-2247; Bogren, Buonocore 1999, pages: 864-866). In 2008 also Frydrychowitz spoke of predominantly right-handed flow in healthy subjects having undergone 4D CMR (Frydrychowicz et al. 2008, page: 401). And in 2010 Hope and associates found right handed flow patterns in 80% of the healthy individuals in their 4D CMR studies when comparing blood flow in ascending aortic aneurysms to healthy aorta (Hope et al. 2007, page: 1475).

Those more dimensional visualisations of blood flow established enormous new knowledge about flow patterns in the AAo. Using 4D CMR Barker and Meierhofer were independently able to demonstrate significantly different flow patterns in BAV compared to TAV (Barker et al. 2010, pages: 793-794; Meierhofer et al. 2010, poster presentation). While right handed flow in healthy subjects with TAV correlated with the findings of the investigators listed before, flow patterns in BAV patients were outstanding different. Moreover, Barker found significantly higher WSS values in the ascending aorta of BAV patients (Barker et al. 2010, pages: 794-795). Complementary to those results, the present study could also show higher wall shear stress in the AAo in two age and sex matched populations with TAV and BAV. Our data reveal that flow despite absence of aortic valve disease like stenosis or regurgitation is significantly different in BAV compared to TAV (*chapter 3*). Moreover, these abnormal flow patterns behind BAV correlate with significantly increased wall shear stress upon the ascending aortic wall.

Facing our data, the author would like to answer the prior introduced question and state that valve shape and opening fashion might certainly have relevance and should also be considered as significant flow disturbing parameters. Furthermore, he would like to suggest that haemodynamic in the ascending aorta in normally functioning BAV were widely underestimated up to date.

In summary, Gunteroth's opinion is not unlikely. Considering existing significantly higher wall shear stress in the middle AAo of BAV patients presented in this work it must be allowed to take higher

WSS in account as a possibly responsible factor for aortic dilation in BAV; likewise increased blood pressure or jets are thought to be causative in aortic dilation and dissection in TAV (Wiener et al. 2004, page: 1483; Bauer et al. 2006, page: 600).

And in deed various studies could demonstrate the influence of wall shear stress on vascular tissue. Hoffman et al. did only recently review how "forces of (…) dynamic characteristics regulate distinct signalling pathways" (Hoffman 2011, page: 316). Davies comprehensively reviewed in 1995 shear stress related responses of endothelial cells (Davies 1995, pages: 536-537) while Garin and Berk concluded in 2006 that shear stress can be sensed by endothelial cells and modulate them by complexly connected signalling (Garin, Berk, page: 381). However, not only endothelial cells but also smooth muscle cells (SMC) and certain enzymes like Matrix-metallo-proteinases (MMP) and extracellular matrix (ECM) are involved (Sakamoto 2006, pages: 412-414; Terada 2008, pages: 562-564).

Especially MMP are in the focus of interest regarding aortic aneurysmal disease where they appear to have deep impact in aneurysmal degeneration (Longo et al. 2002, page: 631). MMP are capable to degrade aortic integrity maintaining components like elastin or collagen (LeMaire et al. 2005, page: 41). But also fibrillin is subject to MMP activity and, as Ashworth et al suggested, might be metabolized by different subtypes of MMP (Ashworth et al. 1999, page: 179). Moreover, up-regulated MMP are thought to play a role in SMC apoptosis (Nataatmadja et al. 2003, page: 329).

The just listed texture features (MMP activity, SMC loss, matrix protein loss) are, surprisingly, exactly the very same which the often citied publications linking BAV with an inborn tissue defect use to defend their theory. Bonderman et al suggested SMC apoptosis to be associated with ascending aortic aneurysm (Bonderman 1999, page: 2142). In 2003, Nataatmadja, referring on Bonderman, wrote that MMP-2 up-regulation might play a role in SMC death in aneurysms (Nataatmadja et al. 2003, page: 329). Structural abnormalities like elastic fragmentation, matrix disruption, fibrillin deficiency similar to MS were seen by Niwa, de Sa and Fedak (Niwa et al. 2001, page: 394; de Sa et al. 1999, page: 590; Fedak et al. 2002, page: 902). Last but not least, Boyum and LeMaire could demonstrate higher levels of MMP activity in ascending aortic aneurysms in BAV patients (Boyum et al. 2004, pages: 689-690; LeMaire et al. 2005, pages: 42-46).

Besides LeMaire and associates who spoke of a combination of congenital tissue abnormality and haemodynamic stress to be causative, none of the other named publications above paid attention to the theory of hydraulic forces like WSS being in charge. Even though, all the latter results in BAV could also be linked to a haemodynamic explanation since shear forces might lead to equal

alterations in vessel tissue (MMP activity, SMC loss, matrix protein loss), subsequently ending in aortic weakness, most authors simply deny this idea.

Based on the findings in this study the author suggests not to completely dismiss a haemodynamic explanation. When looking on the exact study results of the listed publications one may see that most of the wall tissue disorders were not restricted to BAV subjects. Rather, SMC perdition as well as increased MMP activity was also seen in aneurysms of TAV subjects, albeit in lower levels. Interestingly, these wall abnormalities in TAV were not tried to explain with any congenital disorder but were just mentioned (Boyum et al. 2004, pages: 686-691). Proceeding from the assumption that not an inborn defect but haemodynamic forces led to the mentioned wall changes in both BAV and TAV the results might be better understood. While TAV slowly develop haemodynamic disturbances during life, BAV aortas underlie altered haemodynamic from the first day all lifelong.

On the one hand, TAV patients may slightly acquire aging related haemodynamically relevant circumstances in their circulatory system, e.g. arterial HTN or AS, which may impact tissue properties in the AAo. On the other hand, BAV patients do suffer from altered flow forces caused by a differently opening valve from their first heartbeat. Seen from the point of view, that duration of haemodynamic impact matters, the higher levels of texture alterations in BAV patients can be easily explained and do even support a 'haemodynamic theory' of aortic dilation in BAV.

As prior written, Niwa et al could demonstrate tissue abnormalities in BAV aortas similar to those in MS. However, the same study revealed equal findings in the great arterial walls of other CHD, predominantly in those with heavily changed haemodynamic conditions as ventricular septum defect, Tetralogy of Fallot or transposition of the great arteries (Niwa et al. 2001, pages: 393-400). Hence, also these results might be interpreted as flow force effects.

According to Bonderman, Fedak and Nataatmadja, also Cotrufo (Cotrufo et al. 2005, pages: e5-e7) found histologic abnormalities in AAo of BAV subjects. Yet, the uncommon matrix protein patterns were not findable all over the entire circumference of the AAo but especially in their convexity. The same area where aortas with BAV use to dilate most frequently (Bauer et al. 2006, pages: 598-599). Independently, Nkomo could show that echocardiographically measured peak velocities in AAo behind BAV in absence of aortic dilation or severe valve disease were higher than in subjects with TAV (Nkomo et al. 2003, page: 353). And in addition to this, lately, Viscardi et Altera were able to present velocity and flow data from a finite aortic model showing an "asymmetrical distribution of velocity field toward the convexity of the mid-ascending aorta" in bicuspid configurations (Viscardi et al. 2010, pages: 4-6). Also these findings let the theory of haemodynamic stress sound likely.

Looking further back one has to respect the work of Schlatmann et colleagues from the seventies. The investigators clearly describe segmental elastin fragmentation to be a phenomenon occurring normally in the elderly. They constitute that the medial defect in human aortas is due to a "continuous process of injury and repair occurring in the aging aorta" (Schlatmann, Becker 1977b, page: 24). Later they stated the histological changes in the aorta showed "striking correlation to age" (Schlatmann, Becker 1977a, pages: 13, 20). This also stresses the theory of haemodynamic forces. Aortic wall changes appear to be normal side effects of aging. However, they may occur earlier in life when haemodynamic conditions are altered, e.g. in arterial HTN or heavily changed flow forces in BAV.

This assumption of haemodynamic forces causing dilation in a long term process also meets Russo's findings from 2002 when he described more frequent acute aortic events together with larger diameter in BAV patients compared to TAV after aortic valve replacement (AVR) (Russo et al. 2002, page: 1774). AVR was performed at mean age of 50 years in BAV subjects. Assuming from strongly altered flow in BAV those patients must have been suffering from increased shear forces for five decades. The haemodynamic impact upon the aortic wall might have found its effect independently to the replaced valve. Applying these thoughts on Russo's study their results do not appear as striking as argued. And a conclusion of a genetic origin for the findings, like often stated, becomes more unlikely.

These thoughts also meet findings published by others who could show that the most important risk factor for dilation associated with BAV clearly seems to be age (Cecconi et al. 2005, abstract; Della Corte et al. 2007, page: 399; Siu, Silversides 2010, page: 2793).

In 2008, Russo and colleagues contributed another interesting study. They found diverse degrees of wall degeneration and ascending aortic dilation between BAV type 1 and type 2 (classification according to this study). BAV with fused right and left cusp (type 1) revealed statistically higher levels of tissue alterations (Russo et al. 2008, pages: 938-941). A haemodynamic explanation for these results could be the different valve opening fashion, depending on the merged leaflets, with consequently diverse wall shear stress upon the vessel wall. Also the results of the presented study showed different flow characteristics between BAV types one and two (*figure 1*) supporting this explanation. Unfortunately, the amount of data was too little to statistically analyse them.

Apart from that, investigators not only examined aortic wall properties in BAV patients but also tissue of the main pulmonary artery in this population. This was performed as aorta and pulmonary artery arise from the same embryological structure. If the theory of an inborn tissue defect would be

true, wall alterations would also be detectable in both, aorta and MPA of BAV patients. The released data regarding that issue are very interesting.

Kutty was able to show that diameters of the pulmonary artery seem to be larger in subjects with a congenital BAV than in controls. And this appears to happen in absence of pulmonary valve abnormality (Kutty et al. 2010, page: 1756-1757). Supported by these data also Kutty stresses the theory of "primary vessel wall pathology" (Kutty et al. 2010, page: 1758). But, studying the data exactly one can see that the compared populations of BAV subjects and controls were not of the same age. In fact, controls (mean age 9.1 ± 5.7) were significantly younger than BAV patients (mean age 11.5 ±8.38). Facing this, one must ask if the discovered difference in pulmonary artery diameters is not just a matter of age and growth. The author believes that this seems to be the most logical explanation.

Earlier, De Sa and Co could publish that pulmonary autografts after ross procedure in patients with BAV tend to dilate despite replacement of the valve (De Sa et al. 1999, page: 590) and that tissue of the MPA in BAV patients is similarly altered to the ascending aortic wall, also suggesting an inborn defect which affects both the aorta and MPA in BAV subjects. These results have numerously been citied to underscore the theory that primary changes of structural vessel integrity would be the responsible cause for aortic dilation in BAV (Loscalzo et al. 2007, page: 1961). In contrary, Luciani and cowriters did particularly say in their paper from 2000, with regard to de Sa's data, that they could not find the same results and note furthermore that no "correlation between BAV disease, degenerative changes of the pulmonary artery, and autograft root aneurysm has been identified" (Luciani et al. 2001, page: 78). In 2004, Schmid and colleagues concluded their study of structural and biomolecular changes in aorta and pulmonary trunk of patients with aortic aneurysms and valve disease, that "dilation of the pulmonary autograft seems not to be the result of histopathological and biomolecular mechanisms in the pulmonary trunk" (Schmid et al. 2004, abstract). Five years later, Hörer and associates also found different results. They could show that children after undergone Ross procedure do show growth of their neoaortic root, confirming previous findings. However this was not restricted to patients with a bicuspid aortic valve but did affect various populations (Hörer et al. 2009, pages: 594-600).

All together, the postulation of many that De Sa´s and Kutty's works proves a genetic inborn vessel tissue defect in BAV must seriously be reconsidered. Unfortunately, most papers arguing with a genetic disorder of aortic tissue in BAV do simply not mention the results contributed by Luciani, Schmid and Hörer.

Summarizing, despite numerous publications about dilation in BAV there is no evidence of an inborn tissue disorder leading to aortic dilation in patients with BAV. Besides, most papers speaking of an inborn or developmental effect in this pathology use the publications of Bonderman, Fedak, de Sa, Niwa and Hahn to stress their opinion (Bonderman et al. 1999, de Sa et al. 1999, Niwa et al. 2001, Hahn et al. 1992). In fact though, all these papers are lacking of undisputable results. And some data can even be challenged by contrary findings. Moreover, all the citied arguments to prove a genetic defect, like earlier and more frequent widening of the aorta in BAV due to wall abnormalities (SMC loss, elastic degeneration, MMP activity changes) can also logically be reconstructed as results of haemodynamic stress by significantly increased WSS. Supporting that idea, in 2009 Xu and associates evaluated "the association between wall stress and levels of metabolic activities in aneurysms of the descending thoracic and abdominal aorta" pointing to a "potential link between high wall stress and accelerated metabolism in aortic aneurysm wall" (Xu et al. 2009, pages: 295, 300). Bieging et al. just lately discussed that "elevated diastolic shear forces may contribute to aortic aneurysm growth" (Bieging 2011, page: 594).

Thus, the author would clearly like to state the idea of haemodynamic stress leading to dilation in the AAo of BAV patients must not be ruled out.

Nevertheless, highlighting the current knowledge in BAV disease from another point of view does not answer all the questions and some remain unclear. For example, Biner and associates showed that ascending aortic dilation is not only common in BAV patients but also in their first degree relatives (Biner et al. 2009, pages: 4-5). Despite some bias in this work these data deserve respect. Earlier, McKellar et al tried to link occurrence of thoracic aortic aneurysms (TAA) in BAV with *NOTCH1* gene missense variants found in these patients; even though these data were not significant they should not be ignored either (McKellar et al. 2007, pages: 294-295).

In summary, many results in this field of research may be explained with the theory of haemodynamic stress, but the possibility of a genetic tissue disorder cannot totally be denied. The presented study did not aim to finally describe a cause-effect relation of wall shear stress and ascending aortic dilation in BAV patients. Yet, the author intended to enrich the current state of knowledge in this field by contributing new insights into haemodynamic behind BAV and to sceptically review the allegedly overwhelming data often used to underline a theoretically congenital aortic pathology in BAV patients.

However, both theories for dilatation of the ascending aorta in BAV remain theoretical and further research is urgently needed.

4. 6 Conclusion

Concluding, the author would like to complement the quote “Cardiology is flow” (Richter, Edelman 2006, page: 2679): Cardiology, paediatric cardiology and heart surgery are about altered flow and haemodynamical stress.

Many recent studies orientated on flow visualisation and quantification could reveal that flow alterations in cardiovascular disease may be more sophisticated than previously expected (Hope et al. 2007b, pages: 1471-1479; Stalder et al. 2008, pages: 1218-1231). Thus, flow and shear force assessment should be taken into account as a future focus in cardiac diagnostics. The enriching and striking outcomes delivered by 4D CMR are predisposing this method despite its early stage to be an adequate tool for cardiovascular flow force measurement even in clinical routine, e.g. in congenital heart disease or postoperatively in heart surgery.

The presented study of wall shear stress measured in the ascending aorta of BAV patients has shown how effectively this new approach may be applied, and how WSS might be a new “nonsize marker (…) for risk stratification for aortic dissection in patients with BAV” as just recently required by Michelena et al. (Michelena et al. 2011, page: 1111). With regard to the demonstrated results and the still lacking evidence of a supposed intrinsic vessel defect, the author would like to suggest that altered flow conditions followed by increased hemodynamic wall shear stress in BAV must be seen as a determining factor for the development of ascending aortic vessel disease in this population. However, further research is required to define better screening methods and improve risk management as well as therapy strategies for patients with bicuspid aortic valve.

5 Summary

Patients with bicuspid aortic valves (BAV) suffer more often from dilation, aneurysm or dissection of the ascending aorta (AAo) than the normal population. It is commonly known that aortic vessel tissue in BAV patients demonstrates abnormal degeneration processes. However, reasons for that remain unclear. Two opposing theories discuss either an inborn tissue defect or dilation secondary to altered blood flow conditions in the AAo. This topic gains its importance from an 1-2% incidence rate of BAV.

New imaging and flow quantification tools based on cardiovascular magnetic resonance (CMR) developed during the last decade allow for better understanding of blood flow in great vessels. They have revealed that blood flow and blood force alterations may be more severe and sophisticated than expected. By applying these features in assessment of aortic flow it is possible to derive time-resolved three dimensional (4D) flow, velocity and wall shear stress (WSS) data.

Basing on this, this prospective study was initiated to compare shear stress acting upon the ascending aortic wall in BAV patients (n=18) to subjects with tricuspid aortic valve (TAV) (n=18). To avoid confounders study and control population were age and sex matched. Only subjects with normally functioning aortic valve and no haemodynamically relevant disturbances like aortic stenosis, regurgitation or coarctation were included.

Quantification of the acquired 4D CMR data delivered significantly different WSS values ($p = 0.0279$) between BAV subjects and the healthy control population. Despite absence of stenosis or regurgitation, BAV led to strongly altered blood flow resulting in higher haemodynamic stress upon the middle ascending aortic wall in these patients.

Given these results, it can be suggested that shear stress in the ascending aorta of BAV patients has widely been underestimated by many researchers. This argues furthermore for a determining impact of haemodynamic forces in the development of ascending aortic dilation in BAV patients.

4D CMR flow visualization and quantification should be optimized and more intensively applied in flow force assessment to reveal new insights not only in aortic disease of BAV patients but also in many other flow dependent pathologies of the cardiovascular system.

6 Zusammenfassung

Patienten mit bikuspider Aortenklappe (BAV) leiden häufiger an einer Erkrankung der Aorta ascendens (AAo) als die Normalbevölkerung. Auf dem Boden einer Gewebeveränderung der aortalen Gefäßwand kommt es zu öfter zu Dilatation, Aneurysmen bis hin zu Dissektionen der Aorta. Bis heute ist die zu Grunde liegende Pathophysiologie nicht geklärt. Zwei kontrovers diskutierte Theorien sprechen einerseits von einem angeborenen Bindegewebsdefekt, andererseits von einer klappenbedingten hämodynamischen Ursache. Die assoziierten Komplikationen bei einer Inzidenz der BAV von 1-2% machen diese Thematik so bedeutsam.

Basierend auf der kardiovaskulären Magnetresonanz (MR) haben in den vergangenen zehn Jahren entscheidende Weiterentwicklungen auf dem Feld der Flussquantifizierung ein verbessertes Verständnis von Blutfluss in den großen Gefäßen erbracht. Es konnte gezeigt werden, dass Strömungen- und Strömungsveränderungen weit komplexer und komplizierter sind als bisher vermutet. Die zeitlich aufgelöste, dreidimensionale Magnetresonanz (4D MR) ermöglicht es heute, intravasal in vivo Blutfluss-, Geschwindigkeits- und Wandschubspannungsdaten zu gewinnen.

Mittels experimenteller 4D MR konnte die hier beschriebene, prospektive in vivo Studie durchgeführt werden, die Wandschubspannung in der Aorta ascendens bei alters- und geschlechtsgleich akquirierten Patienten mit BAV (n=18) gegenüber gesunden Probanden mit trikuspider Aortenklappe (n=18) vergleicht. Es wurden nur Teilnehmer ohne hämodynamisch relevante Störungen wie Aortenklappenstenose oder -insuffizienz, bekanntem Bindegewebsdefekt, Hypertonie, Aortenisthmusstenose oder anderen Erkrankungen eingeschlossen.

Die Auswertung der generierten Daten wies eine signifikant höhere Wandschubspannung ($p = 0.0279$) bei Patienten mit BAV auf. Obwohl weder Stenose oder Insuffizienz der Klappe, noch Hypertonus oder irgendeine andere kardiale Störung vorlagen, zeigten Patienten mit BAV ein stark verändertes Blutflussmuster in der AAo mit einhergehendem deutlich erhöhtem hämodynamischem Stress auf die aortale Gefäßwand.

Diese Ergebnisse erhärten die Vermutung, dass veränderte Flussmuster samt erhöhtem hämodynamischem Stress einen großen Einfluss auf die Entstehung von Wandveränderungen der AAo bei bikuspider Aortenklappe haben. Des Weiteren zeigt diese Studie erneut, wie nützlich Flussquantifizierung mittels 4D MR zu wissenschaftlichen und zukünftig diagnostischen Zwecken im Rahmen kardiovaskulärer Erkrankungen eingesetzt werden kann.

7 References

Aboulhosn, J.; Child, J. S.: Left ventricular outflow obstruction: subaortic stenosis, bicuspid aortic valve, supravalvar aortic stenosis, and coarctation of the aorta. In: **Circulation (2006), Vol.114, p. 2412–2422**.

ACCF/AHA/AATS/ACR/ASA/SCA/SCAI/SIR/STS/SVM (2010): 2010 ACCF/AHA/AATS/ACR/ASA/SCA/SCAI/SIR/STS/SVM Guidelines for the Diagnosis and Management of Patients With Thoracic Aortic Disease. Online: **http://content.onlinejacc.org/cgi/reprint/55/14/e27.pdf,** last check 27/01/2011.

Amano, Y.; Takagi, R.; Suzuki, Y.; Sekine, T.; Kumita, S.; van Cauteren, M.: Three-dimensional velocity mapping of thoracic aorta and supra-aortic arteries in Takayasu arteritis. In: **J Magn Reson Imaging (2010), Vol.31, p. 1481–1485**.

Ashworth, J. L.; Murphy, G.; Rock, M. J.; Sherratt, M. J.; Shapiro, S. D.; Shuttleworth, C. A.; Kielty, C. M.: Fibrillin degradation by matrix metalloproteinases: implications for connective tissue remodelling. In: **Biochem. J. (1999), Vol.340 (Pt 1), p. 171–181**.

Bammer, R.; Hope, T. A.; Aksoy, M.; Alley, M. T.: Time-resolved 3D quantitative flow MRI of the major intracranial vessels: initial experience and comparative evaluation at 1.5T and 3.0T in combination with parallel imaging. In: **Magn Reson Med (2007), Vol.57, p. 127–140**.

Barker, A. J.; Lanning, C.; Shandas, R.: Quantification of hemodynamic wall shear stress in patients with bicuspid aortic valve using phase-contrast MRI. In: **Ann Biomed Eng (2010), Vol.38, p. 788–800**.

Basso, C.; Boschello, M.; Perrone, C.; Mecenero, A.; Cera, A.; Bicego, D.; Thiene, G.; Dominicis, E. de: An echocardiographic survey of primary school children for bicuspid aortic valve. In: **Am. J. Cardiol. (2004), Vol.93, p. 661–663**.

Bauer, M.; Bauer, U.; Siniawski, H.; Hetzer, R.: Differences in clinical manifestations in patients with bicuspid and tricuspid aortic valves undergoing surgery of the aortic valve and/or ascending aorta. In: **Thorac Cardiovasc Surg (2007), Vol.55, p. 485–490**.

Bauer, M.; Gliech, V.; Siniawski, H.; Hetzer, R.: Configuration of the ascending aorta in patients with bicuspid and tricuspid aortic valve disease undergoing aortic valve replacement with or without reduction aortoplasty. In: **J. Heart Valve Dis. (2006), Vol.15, p. 594–600**.

Bauer, M.; Siniawski, H.; Pasic, M.; Schaumann, B.; Hetzer, R.: Different hemodynamic stress of the ascending aorta wall in patients with bicuspid and tricuspid aortic valve. In: **J Card Surg (2006), Vol.21, p. 218–220**.

Benson, T. J.; Nerem, R. M.; Pedley, T. J.: Assessment of wall shear stress in arteries, applied to the coronary circulation. In: **Cardiovasc. Res. (1980), Vol.14, p. 568–576**.

Bieging, E. T.; Frydrychowicz, A.; Wentland, A.; Landgraf, B. R.; Johnson, K. M.; Wieben, O.; Francois, C. J.: Vivo Three-Dimensional MR Wall Shear Stress Estimation in Ascending Aortic Dilatation. In: **J Magn Reson Imag (2011), Vol.33, p. 589–597**

Biner, S.; Rafique, A. M.; Ray, I.; Cuk, O.; Siegel, R. J.; Tolstrup, K.: Aortopathy is prevalent in relatives of bicuspid aortic valve patients. In: **J. Am. Coll. Cardiol. (2009), Vol.53, p. 2288–2295**.

Bogren, H. G.; Buonocore, M. H.: 4D magnetic resonance velocity mapping of blood flow patterns in the aorta in young vs. elderly normal subjects. In: **J Magn Reson Imaging (1999), Vol.10, p. 861–869**.

Bolton, G. A. A. (2005): Blood flow effects on heart development and a minimally invasive technique for in vivo flow alterations. Online: **http://thesis.library.caltech.edu/1996/1/Acevedo-Bolton_thesis.pdf,** last update 10/05/2005, last check 25/01/2011.

Bonderman, D.; Gharehbaghi-Schnell, E.; Wollenek, G.; Maurer, G.; Baumgartner, H.; Lang, I. M.: Mechanisms underlying aortic dilatation in congenital aortic valve malformation. In: **Circulation (1999), Vol.99, p. 2138–2143**.

Bonow, R. O.: Bicuspid aortic valves and dilated aortas: a critical review of the ACC/AHA practice guidelines recommendations. In: **Am. J. Cardiol. (2008), Vol.102, p. 111–114**.

Bonow, R. O.; Carabello, B. A.; Chatterjee, K.; Leon, A. C. de; Faxon, D. P.; Freed, M. D.; Gaasch, W. H.; Lytle, B. W.; Nishimura, R. A.; O'Gara, P. T.; O'Rourke, R. A.; Otto, C. M.; Shah, P. M.; Shanewise, J. S.; Nishimura, R. A.; Carabello, B. A.; Faxon, D. P.; Freed, M. D.; Lytle, B. W.; O'Gara, P. T.; O'Rourke, R. A.; Shah, P. M.: 2008 focused update incorporated into the ACC/AHA 2006 guidelines for the management of patients with valvular heart disease: a report of the American College of Cardiology/American Heart Association Task Force on Practice Guidelines (Writing Committee to revise the 1998 guidelines for the management of patients with valvular heart disease). Endorsed by the Society of Cardiovascular Anesthesiologists, Society for Cardiovascular Angiography and Interventions, and Society of Thoracic Surgeons. In: **J. Am. Coll. Cardiol. (2008), Vol.52, p. e1-142**.

Botney, M. D.: Role of hemodynamics in pulmonary vascular remodeling: implications for primary pulmonary hypertension. In: **Am. J. Respir. Crit. Care Med. (1999), Vol.159, p. 361–364**.

Boyum, J.; Fellinger, E. K.; Schmoker, J. D.; Trombley, L.; McPartland, K.; Ittleman, F. P.; Howard, A. B.: Matrix metalloproteinase activity in thoracic aortic aneurysms associated with bicuspid and tricuspid aortic valves. In: **J. Thorac. Cardiovasc. Surg. (2004), Vol.127, p. 686–691**.

Braverman, A. C.: Aortic involvement in patients with a bicuspid aortic valve. In: **Heart (2011), Vol.97, p. 506–513**.

Braverman, A. C.; Güven, H.; Beardslee, M. A.; Makan, M.; Kates, A. M.; Moon, M. R.: The bicuspid aortic valve. In: **Curr Probl Cardiol (2005), Vol.30, p. 470–522**.

Bremer (1932): The presence and influence of two spiral streams in the heart of the chick embryo, American Journal of Anatomy - Wiley Online Library. Online: **http://onlinelibrary.wiley.com/doi/10.1002/aja.1000490305/abstract,** last update 25/01/2011, last check 25/01/2011.

Caro, C. G.; Fitz-Gerald, J. M.; Schroter, R. C.: Arterial wall shear and distribution of early atheroma in man. In: **Nature (1969), Vol.223, p. 1159–1160**.

Cecconi, M.; Manfrin, M.; Moraca, A.; Zanoli, R.; Colonna, P. L.; Bettuzzi, M. G.; Moretti, S.; Gabrielli, D.; Perna, G. P.: Aortic dimensions in patients with bicuspid aortic valve without significant valve dysfunction. In: **Am. J. Cardiol. (2005), Vol.95, p. 292–294**.

Cheng, C.; Tempel, D.; van Haperen, R.; van der Baan, A.; Grosveld, F.; Daemen, M. J. A. P.; Krams, R.; Crom, R. de: Atherosclerotic lesion size and vulnerability are determined by patterns of fluid shear stress. In: **Circulation (2006), Vol.113, p. 2744–2753**.

Cheng, C. P.; Parker, D.; Taylor, C. A.: Quantification of wall shear stress in large blood vessels using Lagrangian interpolation functions with cine phase-contrast magnetic resonance imaging. In: **Ann Biomed Eng (2002), Vol.30, p. 1020–1032**.

Chiu, J.-J.; Chien, S.: Effects of disturbed flow on vascular endothelium: pathophysiological basis and clinical perspectives. In: **Physiol. Rev. (2011), Vol.91, p. 327–387**.

Cotrufo, M.; Della Corte, A.; Santo, L. S. de; Quarto, C.; Feo, M. de; Romano, G.; Amarelli, C.; Scardone, M.; Di Meglio, F.; Guerra, G.; Scarano, M.; Vitale, S.; Castaldo, C.; Montagnani, S.:

Different patterns of extracellular matrix protein expression in the convexity and the concavity of the dilated aorta with bicuspid aortic valve: preliminary results. In: **J. Thorac. Cardiovasc. Surg. (2005), Vol.130, p. 504–511**.

Cripe, L.; Andelfinger, G.; Martin, L. J.; Shooner, K.; Benson, D. W.: Bicuspid aortic valve is heritable. In: **J. Am. Coll. Cardiol. (2004), Vol.44, p. 138–143**.

Davies, P. F.: Flow-mediated endothelial mechanotransduction. In: **Physiol. Rev. (1995), Vol.75, p. 519–560**.

Della Corte, A.; Bancone, C.; Quarto, C.; Dialetto, G.; Covino, F. E.; Scardone, M.; Caianiello, G.; Cotrufo, M.: Predictors of ascending aortic dilatation with bicuspid aortic valve: a wide spectrum of disease expression. In: **Eur J Cardiothorac Surg (2007), Vol.31, p. 397-404; discussion 404-5**.

Di Gugliemo, L.; Guttadauro, M.: Aortic stenosis associated with aneurysmal dilatation of the ascending aorta. In: **Acta radiol (1955), Vol.43, p. 437–444**.

Dinsmore, R. E.; Liberthson, R. R.; Wismer, G. L.; Miller, S. W.; Liu, P.; Thompson, R.; McLoud, T. C.; Marshall, J.; Saini, S.; Stratemeier, E. J.: Magnetic resonance imaging of thoracic aortic aneurysms: comparison with other imaging methods. In: **AJR Am J Roentgenol (1986), Vol.146, p. 309–314**.

Edwards, W. D.; Leaf, D. S.; Edwards, J. E.: Dissecting aortic aneurysm associated with congenital bicuspid aortic valve. In: **Circulation (1978), Vol.57, p. 1022–1025**.

Fedak, P. W. M.; Sa, M. P. L. de; Verma, S.; Nili, N.; Kazemian, P.; Butany, J.; Strauss, B. H.; Weisel, R. D.; David, T. E.: Vascular matrix remodeling in patients with bicuspid aortic valve malformations: implications for aortic dilatation. In: **J. Thorac. Cardiovasc. Surg. (2003), Vol.126, p. 797–806**.

Fedak, P. W. M.; Verma, S.; David, T. E.; Leask, R. L.; Weisel, R. D.; Butany, J.: Clinical and pathophysiological implications of a bicuspid aortic valve. In: **Circulation (2002), Vol.106, p. 900–904**.

Fernández, B.; Durán, A. C.; Fernández-Gallego, T.; Fernández, M. C.; Such, M.; Arqué, J. M.; Sans-Coma, V.: Bicuspid aortic valves with different spatial orientations of the leaflets are distinct etiological entities. In: **J. Am. Coll. Cardiol. (2009), Vol.54, p. 2312–2318**.

Fratz, S.; Hess, J.; Schuhbaeck, A.; Buchner, C.; Hendrich, E.; Martinoff, S.; Stern, H.: Routine clinical cardiovascular magnetic resonance in paediatric and adult congenital heart disease: patients, protocols, questions asked and contributions made. In: **J Cardiovasc Magn Reson (2008), Vol.10, p. 46**.

Frydrychowicz, A.; Markl, M.; Harloff, A.; Stalder, A. F.; Bock, J.; Bley, T. A.; Berger, A.; Russe, M. F.; Schlensak, C.; Hennig, J.; Langer, M.: [Flow-sensitive in-vivo 4D MR imaging at 3T for the analysis of aortic hemodynamics and derived vessel wall parameters]. In: **Rofo (2007a), Vol.179, p. 463–472**.

Frydrychowicz, A.; Berger, A.; Russe, M. F.; Stalder, A. F.; Harloff, A.; Dittrich, S.; Hennig, J.; Langer, M.; Markl, M.: Time-resolved magnetic resonance angiography and flow-sensitive 4-dimensional magnetic resonance imaging at 3 Tesla for blood flow and wall shear stress analysis. In: **J. Thorac. Cardiovasc. Surg. (2008), Vol.136, p. 400–407**.

Frydrychowicz, A.; Schlensak, C.; Stalder, A.; Russe, M.; Siepe, M.; Beyersdorf, F.; Langer, M.; Hennig, J.; Markl, M.: Ascending-descending aortic bypass surgery in aortic arch coarctation: four-dimensional magnetic resonance flow analysis. In: **J. Thorac. Cardiovasc. Surg. (2007b), Vol.133, p. 260–262**.

Garin, G.; Berk, B. C.: Flow-mediated signaling modulates endothelial cell phenotype. In: **Endothelium (2006), Vol.13, p. 375–384**.

Goerttler, K.: [Effect of blood flow as a factor on the form of the heart during development]. In: **Beitr Pathol Anat (1955), Vol.115, p. 33–56**.

Guntheroth, W. G.: A critical review of the American College of Cardiology/American Heart Association practice guidelines on bicuspid aortic valve with dilated ascending aorta. In: **Am. J. Cardiol. (2008), Vol.102, p. 107–110**.

Hahn, R. T.; Roman, M. J.; Mogtader, A. H.; Devereux, R. B.: Association of aortic dilation with regurgitant, stenotic and functionally normal bicuspid aortic valves. In: **J. Am. Coll. Cardiol. (1992), Vol.19, p. 283–288**.

He, X.; Ku, D. N.: Pulsatile flow in the human left coronary artery bifurcation: average conditions. In: **J Biomech Eng (1996), Vol.118, p. 74–82**.

Herfkens, R. J.; Higgins, C. B.; Hricak, H.; Lipton, M. J.; Crooks, L. E.; Lanzer, P.; Botvinick, E.; Brundage, B.; Sheldon, P. E.; Kaufman, L.: Nuclear magnetic resonance imaging of the cardiovascular system: normal and pathologic findings. In: **Radiology (1983), Vol.147, p. 749–759**.

Herold, G. et altera. „Innere Medizin 2008“, Hrsg.: Dr. Gerd Herold, Köln, 2007.

Higgins, C. B.; Stark, D.; McNamara, M.; Lanzer, P.; Crooks, L. E.; Kaufman, L.: Multiplane magnetic resonance imaging of the heart and major vessels: studies in normal volunteers. In: **AJR Am J Roentgenol (1984), Vol.142, p. 661–667**.

Hinrichsen, K. V. „Humanembryologie; Lehrbuch und Atlas der vorgeburtlichen Entwicklung des Menschen“, Hrsg.: Hinrichsen, Berlin, 1990.

Hoffman, B. D.; Grashoff, C.; Schwartz, M. A.: Dynamic molecular processes mediate cellular mechanotransduction. In: **Nature (2011), Vol.475, p. 316–323**.

Holman, E.: The obscure physiology of poststenotic dilatation; its relation to the development of aneurysms. In: **J Thorac Surg (1954), Vol.28, p. 109–133**.

Hope, M. D.; Hope, T. A.; Meadows, A. K.; Ordovas, K. G.; Urbania, T. H.; Alley, M. T.; Higgins, C. B.: Bicuspid aortic valve: four-dimensional MR evaluation of ascending aortic systolic flow patterns. In: **Radiology (2010), Vol.255, p. 53–61**.

Hope, T. A.; Markl, M.; Wigström, L.; Alley, M. T.; Miller, D. C.; Herfkens, R. J.: Comparison of flow patterns in ascending aortic aneurysms and volunteers using four-dimensional magnetic resonance velocity mapping. In: **J Magn Reson Imaging (2007a), Vol.26, p. 1471–1479**.

Hope, T. A.; Markl, M.; Wigström, L.; Alley, M. T.; Miller, D. C.; Herfkens, R. J.: Comparison of flow patterns in ascending aortic aneurysms and volunteers using four-dimensional magnetic resonance velocity mapping. In: **J Magn Reson Imaging (2007b), Vol.26, p. 1471–1479**.

Hörer, J.; Hanke T.; Stierle U.; Takkenberg J.J.M.; Bogers A. J. J. C.; Hemmer W.; Rein J. G.; Hetzer R.; Hübler M.; Robinson D. R.; Sievers H.H.; Lange R.: Neoaortic Root Diameters and Aortic Regurgitation in Children After the Ross Operation. In: **Ann Thorac Surg (2009), Vol.88, p. 594-600**.

Huntington, K.; Hunter, A. G.; Chan, K. L.: A prospective study to assess the frequency of familial clustering of congenital bicuspid aortic valve. In: **J. Am. Coll. Cardiol. (1997), Vol.30, p. 1809–1812**.

Keane, M. G.; Wiegers, S. E.; Plappert, T.; Pochettino, A.; Bavaria, J. E.; Sutton, M. G.: Bicuspid aortic valves are associated with aortic dilatation out of proportion to coexistent valvular lesions. In: **Circulation (2000), Vol.102, p. III35-9**.

Kilner, P. J.; Yang, G. Z.; Mohiaddin, R. H.; Firmin, D. N.; Longmore, D. B.: Helical and retrograde secondary flow patterns in the aortic arch studied by three-directional magnetic resonance velocity mapping. In: **Circulation (1993), Vol.88, p. 2235–2247**.

Kim, C.; Cervós-Navarro, J.; Pätzold, C.; Tokuriki, Y.; Takebe, Y.; Hori, K.: In vivo study of flow pattern at human carotid bifurcation with regard to aneurysm development. In: **Acta Neurochir (Wien) (1992), Vol.115, p. 112–117**.

Koullias, G. J.; Korkolis, D. P.; Ravichandran, P.; Psyrri, A.; Hatzaras, I.; Elefteriades, J. A.: Tissue microarray detection of matrix metalloproteinases, in diseased tricuspid and bicuspid aortic valves with or without pathology of the ascending aorta. In: **Eur J Cardiothorac Surg (2004), Vol.26, p. 1098–1103**.

Ku, D. N.; Giddens, D. P.; Zarins, C. K.; Glagov, S.: Pulsatile flow and atherosclerosis in the human carotid bifurcation. Positive correlation between plaque location and low oscillating shear stress. In: **Arteriosclerosis (1985), Vol.1985, p. 293–302**.

Kutty, S.; Kaul, S.; Danford, C. J.; Danford, D. A.: Main pulmonary artery dilation in association with congenital bicuspid aortic valve in the absence of pulmonary valve abnormality. In: **Heart (2010), Vol.96, p. 1756–1761**.

LeMaire, S. A.; Wang, X.; Wilks, J. A.; Carter, S. A.; Wen, S.; Won, T.; Leonardelli, D.; Anand, G.; Conklin, L. D.; Wang, X. L.; Thompson, R. W.; Coselli, J. S.: Matrix metalloproteinases in ascending aortic aneurysms: bicuspid versus trileaflet aortic valves. In: **J. Surg. Res. (2005), Vol.123, p. 40–48**.

Lindsay, J.: Coarctation of the aorta, bicuspid aortic valve and abnormal ascending aortic wall. In: **Am. J. Cardiol. (1988), Vol.61, p. 182–184**.

Longo, G. M.; Xiong, W.; Greiner, T. C.; Zhao, Y.; Fiotti, N.; Baxter, B. T.: Matrix metalloproteinases 2 and 9 work in concert to produce aortic aneurysms. In: **J. Clin. Invest. (2002), Vol.110, p. 625–632**.

Loscalzo, M. L.; Goh, D. L. M.; Loeys, B.; Kent, K. C.; Spevak, P. J.; Dietz, H. C.: Familial thoracic aortic dilation and bicommissural aortic valve: a prospective analysis of natural history and inheritance. In: **Am. J. Med. Genet. A (2007), Vol.143A, p. 1960–1967**.

Luciani, G. B.; Barozzi, L.; Tomezzoli, A.; Casali, G.; Mazzucco, A.: Bicuspid aortic valve disease and pulmonary autograft root dilatation after the Ross procedure: a clinicopathologic study. In: **J. Thorac. Cardiovasc. Surg. (2001), Vol.122, p. 74–79**.

Luo, B.; Yang, X.; Wang, S.; Li, H.; Chen, J.; Yu, H.; Zhang, Y.; Zhang, Y.; Mu, S.; Liu, Z.; Ding, G.: High Shear Stress and Flow Velocity in Partially Occluded Aneurysms Prone to Recanalization. In: **Stroke; a journal of cerebral circulation (2011), p. 745-753.**

Malek, A. M.; Alper, S. L.; Izumo, S.: Hemodynamic shear stress and its role in atherosclerosis. In: **JAMA (1999), Vol.282, p. 2035–2042**.

Markl, M.; Arnold, R.; Hirtler, D.; Zur Muhlen, C. von; Harloff, A.; Langer, M.; Hennig, J.; Frydrychowicz, A.: Three-dimensional flow characteristics in aortic coarctation and poststenotic dilatation. In: **J Comput Assist Tomogr (2009), Vol.33, p. 776–778**.

Markl, M.; Harloff, A.; Bley, T. A.; Zaitsev, M.; Jung, B.; Weigang, E.; Langer, M.; Hennig, J.; Frydrychowicz, A.: Time-resolved 3D MR velocity mapping at 3T: improved navigator-gated assessment of vascular anatomy and blood flow. In: **J Magn Reson Imaging (2007), Vol.25, p. 824–831**.

Markl, M.; Kilner, P. J.; Ebbers, T.: Comprehensive 4D velocity mapping of the heart and great vessels by cardiovascular magnetic resonance. In: **J Cardiovasc Magn Reson (2011), Vol.13, p. 7**.

McBride, K. L.; Garg, V.: Heredity of bicuspid aortic valve: is family screening indicated? In: **Heart (2011), Vol.97, p. 1193–1195**.

McKellar, S. H.; Tester, D. J.; Yagubyan, M.; Majumdar, R.; Ackerman, M.J.; Sundt, T.M. 3rd: Novel Notch1 mutations in patients with bicuspid aortic valve disease and thoracic aortic aneurysms In: **J Thorac. Cardiovasc. Surg. (2007), Vol.134, p. 290-296**.

McKusick, V. A.: Association of congenital bicuspid aortic valve and erdheim's cystic medial necrosis. In: **Lancet (1972), Vol.1, p. 1026–1027**.

McKusick, V. A.; Logue, R. B.; Bahnson, H. T.: Association of aortic valvular disease and cystic medial necrosis of the ascending aorta; report of four instances. In: **Circulation (1957), Vol.16, p. 188–194**.

McNamara, M. T.; Higgins, C. B.: Cardiovascular applications of magnetic resonance imaging. In: **Magn Reson Imaging (1984), Vol.2, p. 167–183**.

Meierhofer, C., Lyko C., Schneider E.P., Hutter A., Stern H., Martinoff St., Hess J., Markl M. and Fratz, S. (2010)**:** Visualization of flow in the ascending aorta: bicuspid aortic valves compared to tricuspid aortic valves. **http://jcmr-online.com/content/13/S1/P384**, last check 18/01/2012.

Michelena, H. I.; Khanna, A. D.; Mahoney, D.; Margaryan, E.; Topilsky, Y.; Suri, R. M.; Eidem, B.; Edwards, W.D.; Sundt, T. M. 3rd; Enriquez-Sarano, M.: Incidence of aortic complications in patients with bicuspid aortic valve. In: **JAMA (2011), Vol. 306, p. 1104-1112.**

Mills, P.; Leech, G.; Davies, M.; Leathan, A.: The natural history of a non-stenotic bicuspid aortic valve. In: **Br Heart J (1978), Vol.40, p. 951–957**.

Mohamed, S. A.; Aherrahrou, Z.; Liptau, H.; Erasmi, A. W.; Hagemann, C.; Wrobel, S.; Borzym, K.; Schunkter, H.; Sievers, H.H.; Erdmann, J.: Novel missense mutations (p.T596M and p.P1797H) in NOTCH1 in patients with bicuspid aortic valve. In: **Biochem Biophys Res Commun. (2006), Vol. 345, p. 1460–1465.**

Myerson, S. (2007): Aortic imaging with CMR University of Oxford Centre for Clinical Magnetic Resonance Research (OCMR). Online: **http://scmr.org/; last check 29/12/2011.**

Nataatmadja, M.; West, M.; West, J.; Summers, K.; Walker, P.; Nagata, M.; Watanabe, T.: Abnormal extracellular matrix protein transport associated with increased apoptosis of vascular smooth muscle cells in marfan syndrome and bicuspid aortic valve thoracic aortic aneurysm. In: **Circulation (2003), Vol.108 Suppl 1, p. II329-34**.

Nerem, R. M.: Vascular fluid mechanics, the arterial wall, and atherosclerosis. In: **J Biomech Eng (1992), Vol.114, p. 274–282**.

Nistri, S.; Sorbo, M. D.; Marin, M.; Palisi, M.; Scognamiglio, R.; Thiene, G.: Aortic root dilatation in young men with normally functioning bicuspid aortic valves. In: **Heart (1999), Vol.82, p. 19–22**.

Niwa, K.; Perloff, J. K.; Bhuta, S. M.; Laks, H.; Drinkwater, D. C.; Child, J. S.; Miner, P. D.: Structural abnormalities of great arterial walls in congenital heart disease: light and electron microscopic analyses. In: **Circulation (2001), Vol.103, p. 393–400**.

Nkomo, V. T.; Enriquez-Sarano, M.; Ammash, N. M.; Melton, L. J.; Bailey, K. R.; Desjardins, V.; Horn, R. A.; Tajik, A. J.: Bicuspid aortic valve associated with aortic dilatation: a community-based study. In: **Arterioscler. Thromb. Vasc. Biol. (2003), Vol.23, p. 351–356**.

Pachulski, R. T.; Weinberg, A. L.; Chan, K. L.: Aortic aneurysm in patients with functionally normal or minimally stenotic bicuspid aortic valve. In: **Am. J. Cardiol. (1991), Vol.67, p. 781–782**.

Pedersen, E. M.; Oyre, S.; Agerbaek, M.; Kristensen, I. B.; Ringgaard, S.; Boesiger, P.; Paaske, W. P.: Distribution of early atherosclerotic lesions in the human abdominal aorta correlates with wall shear stresses measured in vivo. In: **Eur J Vasc Endovasc Surg (1999), Vol.18, p. 328–333**.

Pennell, D. J.; Sechtem, U. P.; Higgins, C. B.; Manning, W. J.; Pohost, G. M.; Rademakers, F. E.; van Rossum, A. C.; Shaw, L. J.; Yucel, E. K.: Clinical indications for cardiovascular magnetic resonance (CMR): Consensus Panel report. In: **Eur. Heart J. (2004), Vol.25, p. 1940–1965**.

Rao, P.S.; Coarctation of the aorta. In: **Current Cardiology reports (2005), Vol. 7, p. 425-434.**

Rebergen, S. A.; van der Wall, E. E.; Doornbos, J.; Roos, A. de: Magnetic resonance measurement of velocity and flow: technique, validation, and cardiovascular applications. In: **Am. Heart J. (1993), Vol.126, p. 1439–1456**.

Reid, R. T. W.: Bicuspid aortic valve associated with aneurysmal dilatation of the ascending aorta. In: **Med. J. Aust. (1952), Vol.2, p. 628–629**.

Renz-Polster, H.; Krautzig, St. (Hg.)**: „**Basislehrbuch Innere Medizin. kompakt - greifbar – verständlich“; mit StudentConsult-Zugang. Hrsg.: Renz-Polster, Krautzig, Braun. Urban & Fischer Verlag bei Elsevier, München, 2008.

Richter, Y.; Edelman, E. R.: Cardiology is flow. In: **Circulation (2006), Vol.113, p. 2679–2682**.

Ridgway, J. P.: Cardiac magnetic resonance physics for clinicians: part I. In: **J Cardiovasc Magn Reson (2010), Vol.12, p. 71**.

Roberts, C. S.; Roberts, W. C.: Dissection of the aorta associated with congenital malformation of the aortic valve. In: **J. Am. Coll. Cardiol. (1991), Vol.17, p. 712–716**.

Roberts, W. C.: The congenitally bicuspid aortic valve. A study of 85 autopsy cases. In: **Am. J. Cardiol. (1970), Vol.26, p. 72–83**.

Robicsek, F.; Thubrikar, M. J.; Cook, J. W.; Fowler, B.: The congenitally bicuspid aortic valve: how does it function? Why does it fail? In: **Ann. Thorac. Surg. (2004), Vol.77, p. 177–185**.

Roman, M. J.; Devereux, R. B.; Kramer-Fox, R.; O'Loughlin, J.: Two-dimensional echocardiographic aortic root dimensions in normal children and adults. In: **Am. J. Cardiol. (1989), Vol.64, p. 507–512**.

Russo, C. F.; Cannata, A.; Lanfranconi, M.; Vitali, E.; Garatti, A.; Bonacina, E.: Is aortic wall degeneration related to bicuspid aortic valve anatomy in patients with valvular disease? In: **J. Thorac. Cardiovasc. Surg. (2008), Vol.136, p. 937–942**.

Russo, C. F.; Mazzetti, S.; Garatti, A.; Ribera, E.; Milazzo, A.; Bruschi, G.; Lanfranconi, M.; Colombo, T.; Vitali, E.: Aortic complications after bicuspid aortic valve replacement: long-term results. In: **Ann. Thorac. Surg. (2002), Vol.74, p. S1773-6; discussion S1792-9**.

Sa, M. de; Moshkovitz, Y.; Butany, J.; David, T. E.: Histologic abnormalities of the ascending aorta and pulmonary trunk in patients with bicuspid aortic valve disease: clinical relevance to the ross procedure. In: **J. Thorac. Cardiovasc. Surg. (1999), Vol.118, p. 588–594**.

Schaefer, B. M.; Lewin, M. B.; Stout, K. K.; Gill, E.; Prueitt, A.; Byers, P. H.; Otto, C. M.: The bicuspid aortic valve: an integrated phenotypic classification of leaflet morphology and aortic root shape. In: **Heart (2008), Vol.94, p. 1634–1638**.

Schaefer, B. M.; Lewin, M. B.; Stout, K. K.; Byers, P. H.; Otto, C. M.: Usefulness of bicuspid aortic valve phenotype to predict elastic properties of the ascending aorta. In: **Am. J. Cardiol. (2007), Vol.99, p. 686–690**.

Schievink, W. I.; Mokri, B.: Familial aorto-cervicocephalic arterial dissections and congenitally bicuspid aortic valve. In: **Stroke (1995), Vol.26, p. 1935–1940**.

Schlatmann, T. J.; Becker, A. E.: Histologic changes in the normal aging aorta: implications for dissecting aortic aneurysm. In: **Am. J. Cardiol. (1977a), Vol.39, p. 13–20**.

Schlatmann, T. J.; Becker, A. E.: Pathogenesis of dissecting aneurysm of aorta. Comparative histopathologic study of significance of medial changes. In: **Am. J. Cardiol. (1977b), Vol.39, p. 21–26**.

Schlesinger, A. E.; Hernandez, R. J.: Magnetic resonance imaging in congenital heart disease in children. In: **Tex Heart Inst J (1996), Vol.23, p. 128–143**.

Schmid, F.-X.; Bielenberg, K.; Holmer, S.; Lehle, K.; Djavidani, B.; Prasser, C.; Wiesenack, C.; Birnbaum, D.: Structural and biomolecular changes in aorta and pulmonary trunk of patients with aortic aneurysm and valve disease: implications for the Ross procedure. In: **Eur J Cardiothorac Surg (2004), Vol.25, p. 748–753**.

Schmid, F.-X.; Bielenberg, K.; Schneider, A.; Haussler, A.; Keyser, A.; Birnbaum, D.: Ascending aortic aneurysm associated with bicuspid and tricuspid aortic valve: involvement and clinical relevance of smooth muscle cell apoptosis and expression of cell death-initiating proteins. In: **Eur J Cardiothorac Surg (2003), Vol.23, p. 537–543**.

Shojima, M.; Oshima, M.; Takagi, K.; Torii, R.; Hayakawa, M.; Katada, K.; Morita, A.; Kirino, T.: Magnitude and role of wall shear stress on cerebral aneurysm: computational fluid dynamic study of 20 middle cerebral artery aneurysms. In: **Stroke (2004), Vol.35, p. 2500–2505**.

Simon, J. (2010): 3D-Strömungsanalyse der Aorta mittels 3Tesla Magnetresonanztomographie - Rolle des retrograden Flusses und der Wand-schubspannung für die Schlaganfallentstehung. Online: **http://www.freidok.uni-freiburg.de/volltexte/7840/pdf/DissertationJanSimon.pdf,** last check 18/01/2012.

Siu, S. C.; Silversides, C. K.: Bicuspid aortic valve disease. In: **J. Am. Coll. Cardiol. (2010), Vol.55, p. 2789–2800**.

Stalder, A. F.; Russe, M. F.; Frydrychowicz, A.; Bock, J.; Hennig, J.; Markl, M.: Quantitative 2D and 3D phase contrast MRI: optimized analysis of blood flow and vessel wall parameters. In: **Magn Reson Med (2008), Vol.60, p. 1218–1231**.

Stalder, A. F. (2009): Quantitative analysis of blood flow and vessel wall parameters using 4D flow-sensitive MRI. **http://www.freidok.uni-freiburg.de/volltexte/6428/**, last check: 18.01.2012.

Stein, P. D.; Sabbah, H. N.: Turbulent blood flow in the ascending aorta of humans with normal and diseased aortic valves. In: **Circ. Res. (1976), Vol.39, p. 58–65**.

Terada, L. S.: What underlies endothelial shear sensing? The matrix, of course. In: **Circ. Res. (2008), Vol.103, p. 562–564**.

Tse, K. M.; Chiu, P.; Lee, H. P.; Ho, P.: Investigation of hemodynamics in the development of dissecting aneurysm within patient-specific dissecting aneurismal aortas using computational fluid dynamics (CFD) simulations. In: **Journal of biomechanics (2011), Vol. 44, p. 827-836.**

Unterhinninghofen, R.; Ley, S.; Frydrychowicz, A.; Markl, M.: [MR-based tridirectional flow imaging. Acquisition and 3D analysis of flows in the thoracic aorta]. In: **Radiologe (2007), Vol.47, p. 1012–1020**.

Varaprasathan, G. A.; Araoz, P. A.; Higgins, C. B.; Reddy, G. P.: Quantification of flow dynamics in congenital heart disease: applications of velocity-encoded cine MR imaging. In: **Radiographics (2002), Vol.22, p. 895-905; discussion 905-6**.

Viscardi, F.; Vergara, C.; Antiga, L.; Merelli, S.; Veneziani, A.; Puppini, G.; Faggian, G.; Mazzucco, A.; Luciani, G. B.: Comparative Finite Element Model Analysis of Ascending Aortic Flow in Bicuspid and Tricuspid Aortic Valve. In: **Artificial organs (2010), Vol. 34, p. 1114-1120.**

Ward, C.: Clinical significance of the bicuspid aortic valve. In: **Heart (2000), Vol.83, p. 81–85**.

Wentzel, J. J.; Corti, R.; Fayad, Z. A.; Wisdom, P.; Macaluso, F.; Winkelman, M. O.; Fuster, V.; Badimon, J. J.: Does shear stress modulate both plaque progression and regression in the thoracic aorta? Human study using serial magnetic resonance imaging. In: **J. Am. Coll. Cardiol. (2005), Vol.45, p. 846–854**.

Wetzel, S.; Meckel, S.; Frydrychowicz, A.; Bonati, L.; Radue, E.-W.; Scheffler, K.; Hennig, J.; Markl, M.: In vivo assessment and visualization of intracranial arterial hemodynamics with flow-sensitized 4D MR imaging at 3T. In: **AJNR Am J Neuroradiol (2007), Vol.28, p. 433–438**.

Wiener, C. M.; Kasper, D. L.; Braunwald, E.; Fauci, A.; Hauser, S. L.; Longo, D. L.; Jameson, J. L**.: "**Harrisons Principles of Internal Medicine Board Review": Self-assessment and Board Review. McGraw-Hill Medical, New York, 2008.

Wood, J. C.: Anatomical assessment of congenital heart disease. In: **J Cardiovasc Magn Reson (2006), Vol.8, p. 595–606**.

Xu, X. Y.; Borghi, A.; Nchimi, A.; Leung, J.; Gomez, P.; Cheng, Z.; Defraigne, J.O.; Sakalihasan, N.: High levels of 18F-FDG uptake in aortic aneurysm wall are associated with high wall shear stress. In: **Eur J Vasc Endovasc Surg (2010), Vol. 39, p. 295–301.**

Zarins, C. K.; Giddens, D. P.; Bharadvaj, B. K.; Sottiurai, V. S.; Mabon, R. F.; Glagov, S.: Carotid bifurcation atherosclerosis. Quantitative correlation of plaque localization with flow velocity profiles and wall shear stress. In: **Circ. Res. (1983), Vol.53, p. 502–514**.

8 Figures

9 Tables

Acknowledgement

I would like to thank both Prof. John Hess, PhD, as well as Dr. Stefan Martinoff, MD, for the opportunity to perform the presented scientific work in their Department of Paediatric Cardiology and Congenital Heart Disease and the Institute of Radiology at the German Heart Centre Munich, Germany.

My extraordinary thanks go to my supervisors Heiko Stern, PhD, Christian Meierhofer, MD, and of course particularly to Sohrab Fratz, PhD, for their continuous assistance and help during the last three years.

I also want to thank Christine Lyko, MD, Henrike Rieger, MD, Ramona Lorenz, M.Sc., Alred Hager, PhD, Andrea Hutter, MD, Michael Markl, PhD, and my very good friend Maria Zywica, MD for their contributed inputs and important co-work on the project.

Special thanks deserve all the patients and volunteers for their unselfish cooperation on the study.

Very many thanks go to my family, especially my mother, for their everlasting support.

And, last but not least, I would like to thank Dr. Hasenbein.